CIVIL ENGINEERING STUDIES
STRUCTURAL RESEARCH SERIES NO. 89

A STUDY OF BLAST LOADING TRANSMITTED TO BUILDING FRAMES

By
W. J. FRANCY
and
N. M. NEWMARK

Technical Report
to
OFFICE OF NAVAL RESEARCH
Contract N6ori-071(06), Task Order VI
Project NR-064-183

UNIVERSITY OF ILLINOIS
URBANA, ILLINOIS

A STUDY OF BLAST LOADING TRANSMITTED TO BUILDING FRAMES

by

W. J. Francy and N. M. Newmark

A Technical Report of a Research Program

Sponsored by

THE OFFICE OF NAVAL RESEARCH
DEPARTMENT OF THE NAVY

In Cooperation With

THE DEPARTMENT OF CIVIL ENGINEERING
UNIVERSITY OF ILLINOIS

Contract N6ori-071(06), Task Order VI
Program NR-064-183

Urbana, Illinois
December 1954

CONTENTS

ACKNOWLEDGMENT

The author wishes to thank Professor N. M. Newmark, Research Professor of Structural Engineering at the University of Illinois, for his guidance and encouragement during the preparation of this thesis, and to express his appreciation to Professor L. E. Goodman, formerly of the University of Illinois, for his many helpful suggestions and criticisms.

A STUDY OF BLAST LOADING TRANSMITTED TO BUILDING FRAMES

I. INTRODUCTION

A. Introductory Statement

The loading which a structure experiences due to the pressure waves accompanying blasts from high explosive and atomic bombs has been the subject of much study and research since the use of such bombs was begun in the last war. The advent of more powerful atomic bombs and of the "super" bombs has increased even more the urgency of discovering with greater exactness the nature of blast loads on structures.

A recent study in the field of blast loading[1] has concluded that a generalized triangular pulse is a good approximation to the actual transient loads which the front wall of a structure experiences. However depending on the action of the wall covering, the shape of the load-time curves that reach the building frame itself may be quite different from the pulse which impinges on the wall panels. It is the purpose of this thesis to study the load-time relationship for the load transmitted by the wall covering to the supporting frame.

The problem is necessarily complex and is approached by making use of certain simplifying assumptions. The most important are:

(1) Given a typical bay of a one-story frame-type building, consider that the wall covering of the bay consists of a "nest" of closely-spaced beams of unit width which are simply supported and act

---

[1] N. M. Newmark, "An Engineering Approach to Blast Resistant Design", Proceedings ASCE, Vol. 79, Separate No. 306, October 1953.

independently of one another. (Figure 1) These beams are used in this study to approximate the action of a slab covering.

(2) Assume that the pressure loading which impinges on the wall panels can be represented by a triangular pulse function.[2] (Figure 2)

(3) Assume ideal elasto-plastic action of the beams. (Figure 3)

(4) Assume that the frame members supporting the wall covering remain fixed in space, at least during the interval for which this study is made.

It is doubtful that movement of the frame would have much effect on the loads reaching the frame members. A deflection of the frame away from the blast source would result in a slight decrease in the beam end reactions; but, since the period of vibration of the supports is much larger than that of the wall panels, the effect should be negligible except possibly for load pulses of very long duration.

If the beams which approximate the wall covering were perfectly rigid and massless, the shape of the load transmitted to the frame would be identical to that of the blast pressure pulse (Figure 2). However in our case, the beams have mass and also have elasto-plastic characteristics; therefore, the load which reaches the supporting members is much altered.

In order to determine the frame loading for the given assumptions, an elastic analysis and a simple plastic analysis are used. The elastic analysis is derived from the familiar dynamic beam equation (1) and the plastic one comes from a simplified consideration of beam action when a

---

[2] N. M. Newmark, "An Engineering Approach to Blast Resistant Design", Proceedings ASCE, Vol. 79, Separate No. 306, October 1953.

plastic hinge forms at the center. From these two analyses expressions for the dynamic end reaction of the beams on the supports are derived.

Frame load charts giving the variation of dynamic end reaction (frame load per unit height) with respect to time are drawn for different beam resistance characteristics and different load pulse durations. The frame loads are compared graphically with the load which the beam receives as a result of the blast pressure wave. Load-time curves for the supporting frame are shown only for the duration of the loading pulse; however, a method is indicated by which the relation may be found for times beyond the end of the pulse.

As brought out in a subsequent section of this study, the elastic reaction expression involves the sum of a trigonometric series. For certain durations of loading pulses, the curves for one term, three terms and six terms are drawn for comparison. By means of this graphical comparison of a few representative pulse durations, it is demonstrated that the use of only the first term gives results which are fairly accurate for long pulses but not very accurate for short pulses. For all the remaining pulse durations, only the first mode (one term) is used although this is only an approximation to the exact relation which theoretically would require an infinite number of terms. No attempt is made by analytical means to evaluate the accuracy obtainable for various pulse durations by using only the first mode. Such an evaluation could be made the subject of further study. The advantages of using the first mode approximation in the construction of the frame load charts is apparent, however, and such use is intended.

B. Notation

Terms used in the following sections are defined as they appear. They are assembled here for convenience in reference. Dimensions of the quantities are indicated by the symbols F, M, L, T in parentheses meaning respectively force, mass, length and time.

a^2 = EI/m (L^4/T^2)

θ = angular displacement

$\dot{\theta}$ = angular velocity $(1/T)$

$\ddot{\theta}$ = angular acceleration $(1/T^2)$

I = impulse of load = $\int_0^{t_1} p\,dt$ (FT/L)

$\varphi(t)$ = time distribution factor

K = $1/(t_1/T_1)$

ℓ = length of beam (wall panel strip) (L)

m = mass per unit length of beam (M)

M_D = dynamic bending moment at center of beam (FL)

M_P = fully plastic moment of beam (FL)

M_S = maximum static center moment = $P_m\ell^2/8$ (FL)

M_U = ultimate moment - carrying capacity of beam (FL)

p = instantaneous value of applied pressure load (F/L)

$p(x) = \sum_n^{\infty} P_n X_n$ = space distribution factor

P_m = maximum value of applied pressure load (F/L)

R_D = dynamic end reaction (F)

R_S = maximum static end reaction = $P_m\ell/2$ (F)

t = time (T)

t_1 = duration of load pulse (T)

t_e = time of beginning of elastic recovery phase (T)

t_p = time of beginning of plastic phase (T)

t' = $t-t_p$ (T)

t'' = $t-t_e$ (T)

T_n = natural periods of vibration of beam (T)

T_1 = fundamental natural period of vibration of beam (T)

τ_n = a function of time alone

V = shear (F)

w = deflection of beam (L)

$\dot{w}$ = linear velocity of beam (L/T)

$\bar{w}$ = displacement of mass center from axis of rotation (L)

$\ddot{\bar{w}}$ = acceleration of mass center (L/T^2)

$\bar{w}_{c_e}$ = effective center deflection of beam at onset of elastic recovery phase (L)

w_{c_m} = maximum center deflection of beam which occurs at $t = t_e$ (L)

w_y = center deflection of beam at $t = t_p$ (L)

X_n = characteristic function for beam

ω_n = natural (circular) frequencies of beam = $\frac{n^2\pi^2}{\ell^2}\sqrt{\frac{EI}{m}}$ (1/T)

ω_1 = fundamental natural frequency of beam (1/T)

II. INITIAL ELASTIC BEHAVIOR OF WALL PANELS

A. Statement of the Problem

1. The Dynamic Beam Equation[3]

When a beam resists moving loads, the governing differential equation of motion for the beam is, according to the ordinary Bernoulli-Euler theory of flexure,

$$a^2 \frac{\partial^4 w}{\partial x^4} + \frac{\partial^2 w}{\partial t^2} = \frac{p}{m} = \frac{p(x)\,\varphi(t)}{m} = \frac{\sum_{n}^{\infty} P_n X_n \varphi(t)}{m} \qquad (1)$$

where $a^2 = EI/m$; w = deflection measured normal to the beam axis; m = mass per unit length; p = external applied unit load; x = distance measured from origin at left end of beam; and t = time. The external applied load is defined by a space distribution factor, $p(x) = \sum_{n}^{\infty} P_n X_n$ and a time distribution factor, $\varphi(t)$. Figure 4 is a simplified sketch of the loading on a typical beam. For the given triangular loading pulse, $p(x) = 1$ since the beam is assumed to be uniformly loaded, and $\varphi(t) = P_m(1 - t/t_1)$. The characteristic function, X_n, for a simply supported beam is $\sin(n\pi x/\ell)$. The constants, P_n, are defined as:

$$P_n = \frac{\int_0^{\ell} p(x)\, X_n\, dx}{\int_0^{\ell} X_n^2\, dx} \qquad (2)$$

Substituting in (2) and performing the integrations leads to:

$$P_n = \frac{4}{n\pi} \text{ for } n = 1, 3, 5, 7 \ldots\ldots$$

$$P_n = 0 \text{ for } n = 0, 2, 4, 6 \ldots\ldots$$

---

(3) See for example, S. Timoshenko, "Vibration Problems in Engineering", D. Van Nostrand Co., Inc., New York, N. Y., Second Edition, July 1937, p. 332.

The solution to (1) is taken in the form

$$w = \sum_{n}^{\infty} X_n \tau_n \tag{3}$$

where $X_n = \sin (n\pi x/\ell)$, a function of x alone, and where τ_n is a function of time alone. The substitution of (3) in (1) with the subsequent separation of variables leads to the following differential equations:

$$X_n'''' - \frac{\omega_n^2 X_n}{a^2} = 0 \tag{4}$$

$$\ddot{\tau}_n + \omega_n^2 \tau_n = \frac{P_n \varphi(t)}{m} \tag{5}$$

The solutions of (4) and (5) are respectively:

$$X_n = \sin \frac{n\pi x}{\ell} \qquad \text{(always true for simply-supported beam)} \tag{6}$$

$$\tau_n = A_n \cos \omega_n t + B_n \sin \omega_n t$$

$$+ \frac{P_n}{m\omega_n} \left[\sin \omega_n t \int_0^t \varphi(t) \cos \omega_n t dt - \cos \omega_n t \int_0^t \varphi(t) \sin \omega_n t dt \right] \tag{7}$$

Equation (7) is the solution to the single-degree of freedom Equation (5).[4] The first two terms in (7) are the free vibration terms and the last two the forced vibration terms. For initial conditions of zero displacement and zero velocity, the free vibration terms disappear since

---

[4] S. Timoshenko, "Vibration Problems in Engineering", D. Van Nostrand Co., Inc., New York, N. Y., Second Edition, July 1937, p. 348.

$$A_n = \frac{\int_0^{\ell} w_o(x)\, X_n\, dx}{\int_0^{\ell} X_n^{\,2}\, dx}$$

$$B_n = \frac{1}{\omega_n} \frac{\int_0^{\ell} \dot{w}_o(x)\, X_n\, dx}{\int_0^{\ell} X_n^{\,2}\, dx}$$

where $w_o(x)$ and $\dot{w}_o(x)$ are the displacement and velocity respectively at zero time.

Substituting Equations (6) and (7) into the expression for deflection (3), yields the following:

$$w = \sum_n^{\infty} \frac{P_n}{m\omega_n} \sin \frac{n\pi x}{\ell} \left[\sin \omega_n t \int_0^t \varphi(t) \cos \omega_n t\, dt - \cos \omega_n t \int_0^t \varphi(t) \sin \omega_n t\, dt \right] \quad (8)$$

Substituting the values of P_n and $\varphi(t)$ in (8) and integrating, results in the following expression for w:

$$w = \sum_n^{\infty} \frac{4}{n\pi} \frac{1}{m\omega_n} \frac{P_m}{\omega_n} \sin \frac{n\pi x}{\ell} \left[(1 - \cos \omega_n t) - \frac{t}{t_1} \left(1 - \frac{\sin \omega_n t}{\omega_n t} \right) \right]$$

Noting that ω_n for a simply-supported beam = $(n^2\pi^2/\ell^2)\, a$, where $a = \sqrt{EI/m}$:

$$w = \frac{4P_m \ell^4}{\pi^5 EI} \sum_{n=1,3,5\text{---}}^{\infty} \frac{1}{n^5} \sin \frac{n\pi x}{\ell} \left[(1 - \cos \omega_n t) - \frac{t}{t_1} \left(1 - \frac{\sin \omega_n t}{\omega_n t} \right) \right] \quad (9)$$

B. Reaction and Moment Expressions

1. Dynamic End Reaction

The shear at any point x along the beam is given by:

$$V = - EI \frac{\partial^3 w}{\partial x^3}$$

Performing the differentiation on (9) and evaluating the expression at the end of the beam (x = 0), the dynamic end reaction is:

$$R_D = \frac{4P_m \ell}{\pi^2} \sum_{n=1,3,5---}^{\infty} \frac{1}{n^2} \left[(1 - \cos \omega_n t) - \frac{t}{t_1} \left(1 - \frac{\sin \omega_n t}{\omega_n t} \right) \right]$$

If P_m, the maximum value of the external load, were applied as a static load, the maximum static end reaction would be:

$$R_S = \frac{P_m \ell}{2}$$

For ease in plotting, the reaction expression is put into dimensionless form by noting that $\omega_n = 2\pi/T_n = 2\pi n^2/T_1$ since $T_n = T_1/n^2$.

$$\frac{R_D}{R_S} = \frac{8}{\pi^2} \sum_{n=1,3,5---}^{\infty} \frac{1}{n^2} \left[\left(1 - \cos 2\pi n^2 \frac{t}{T_1} \right) - 1/(t_1/T_1) \cdot t/T_1 \left(1 - \frac{\sin 2\pi n^2 \, t/T_1}{2\pi n^2 \, t/T_1} \right) \right] \quad (1$$

2. Magnitude of Reaction for Long Pulses

As the duration of the load pulse goes to infinity, the coefficient of the second term in (10) approaches zero and the reaction approaches:

$$\lim \frac{R_D}{R_S} = \frac{8}{\pi^2} \sum_{n=1,3,5\text{---}}^{\infty} \frac{1}{n^2} \left(1 - \cos 2\pi n^2 \frac{t}{T_1} \right)$$

$$t_1/T_1 \longrightarrow \infty$$

The maximum reaction then approaches:

$$\lim \frac{8}{\pi^2} \sum_{n=\text{odd}}^{\infty} \frac{2}{n^2} = \lim \frac{16}{\pi^2} \sum_{n=\text{odd}}^{\infty} \frac{1}{n^2} \text{, where } \lim \sum_{n=\text{odd}}^{\infty} \frac{1}{n^x} = \left(1 - 2^{-x} \right) \xi(x)$$

The limit of the summation exists as shown. It is given by the Riemann Zeta Function, the values of which are tabulated.(5)

For $x = 2$, $\xi(2) = \pi^2/6 = 1.645$; or:

$$\lim \frac{R_D}{R_S} = \lim \frac{16}{\pi^2} \sum_{n=\text{odd}}^{\infty} \frac{1}{n^2} = \frac{16}{\pi^2} \left[(1 - 1/4) \frac{\pi^2}{6} \right] = 2.00$$

$$t_1/T_1 \longrightarrow \infty$$

Then for pulses of duration approaching infinity, the dynamic reaction approaches a value twice the maximum static reaction. This result is to be expected from energy considerations.

(5) E. Jahnke and F. Emde, "Tables of Functions with Formulae and Curves", Dover Publications, New York, N. Y., Fourth Edition, 1943.

3. Magnitude of Reaction for Short Pulses and Constant Impulse

For short pulses of duration approaching zero, the reaction should also approach a limit. This limit can be found from a consideration of the reaction expression which holds for time beyond the end of the pulse as the pulse duration becomes very small and total impulse remains constant. Figure 5 shows the new time origin at $t = t_1$.

As before, the deflection, $w = \sum_n^{\infty} X_n \tau_n$. However for $t > t_1$, the forced vibration terms in τ_n drop out, leaving:

$$\tau_n = A_n \cos \omega_n t^* + B_n \sin \omega_n t^*$$

The initial conditions of displacement and velocity for $t^* = 0$ can be found from Equation (9). Setting $t = t_1$ in (9):

$$w_o(x) = \frac{4P_m \ell^4}{\pi^5 EI} \sum_{n=odd}^{\infty} \frac{1}{n^5} \sin \frac{n\pi x}{\ell} \left[\frac{\sin \omega_n t_1}{\omega_n t_1} - \cos \omega_n t_1 \right]$$

Differentiating (9) with respect to time and setting $t = t_1$:

$$\dot{w}_o(x) = \frac{4P_m \ell^4}{\pi^5 EI} \sum_{n=odd}^{\infty} \frac{1}{n^5} \sin \frac{n\pi x}{\ell} \left[\omega_n \sin \omega_n t_1 + \frac{\cos \omega_n t_1}{t_1} - \frac{1}{t_1} \right]$$

Values of A_n and B_n are then:

$$A_n = \frac{\int_0^{\ell} w_o(x)\, X_n\, dx}{\int_0^{\ell} X_n^{\,2}\, dx} \qquad \text{where } X_n = \sin \frac{n\pi x}{\ell}$$

$$A_n = \frac{4P_m \ell^4}{\pi^5 EI} \sum_{n=\text{odd}}^{\infty} \frac{1}{n^5} \left[\frac{\sin \omega_n t_1 - \omega_n t_1 \cos \omega_n t_1}{\omega_n t_1} \right]$$

$$B_n = \frac{1}{\omega_n} \frac{\int_0^{\ell} \dot{w}_o(x)\, X_n\, dx}{\int_0^{\ell} X_n^{\,2}\, dx}$$

$$B_n = \frac{4P_m \ell^4}{\pi^5 EI} \sum_{n=\text{odd}}^{\infty} \frac{1}{n^5} \left[\frac{\omega_n t_1 \sin \omega_n t_1 + \cos \omega_n t_1 - 1}{\omega_n t_1} \right]$$

Then for $t^* = t - t_1$:

$$w(x) = \frac{4P_m \ell^4}{\pi^5 EI} \sum_{n=\text{odd}}^{\infty} \frac{1}{n^5} \sin \frac{m\pi x}{\ell} \left[\cos \omega_n t^* \left(\frac{\sin \omega_n t_1 - \omega_n t_1 \cos \omega_n t_1}{\omega_n t_1} \right) \right.$$

$$\left. + \sin \omega_n t^* \left(\frac{\omega_n t_1 \sin \omega_n t_1 + \cos \omega_n t_1 - 1}{\omega_n t_1} \right) \right]$$

As before, find the shear and evaluate at x = 0 in order to get the dynamic end reaction:

$$R_D = \frac{4P_m \ell}{\pi^2} \sum_{n=odd}^{\infty} \frac{1}{n^2} \left[\cos \omega_n t^* \left(\frac{\sin \omega_n t_1 - \omega_n t_1 \cos \omega_n t_1}{\omega_n t_1} \right) \right.$$

$$\left. + \sin \omega_n t^* \left(\frac{\omega_n t_1 \sin \omega_n t_1 + \cos \omega_n t_1 - 1}{\omega_n t_1} \right) \right] \qquad (11)$$

For any pulse duration, the impulse of the load is:

$$I = \int_0^{t_1} p dt = 1/2 \, P_m t_1$$

Now let $t_1 \longrightarrow 0$ keeping the total impulse constant. P_m then increases rapidly, and in terms of I is given by:

$$P_m = \frac{2I}{t_1}$$

Replacing P_m in (11) by its value in terms of I and taking t_1 inside the summation:

$$R_D = \frac{8I\ell}{\pi^2} \sum_{n=odd}^{\infty} \frac{1}{n^2} \left[\cos \omega_n t^* \left(\frac{\sin \omega_n t_1 - \omega_n t_1 \cos \omega_n t_1}{\omega_n t_1^2} \right) \right.$$

$$\left. + \sin \omega_n t^* \left(\frac{\omega_n t_1 \sin \omega_n t_1 + \cos \omega_n t_1 - 1}{\omega_n t_1^2} \right) \right]$$

Now let t_1 approach zero:

$$\lim_{t_1 \longrightarrow 0} R_D = \frac{8I\ell}{\pi^2} \sum_{n=odd}^{\infty} \frac{1}{n^2} \frac{\omega_n}{2} \sin \omega_n t^* = \frac{4I\ell}{\pi^2} \sum_{n=odd}^{\infty} \frac{\omega_n}{n^2} \sin \omega_n t^*$$

Noting again that $\omega_n = 2\pi/T_n$ and replacing I by $(1/2)\, P_m\, t_1$:

$$\lim_{t_1 \longrightarrow 0} \frac{R_D}{R_S} = \frac{8t_1}{\pi} \sum_{n=odd}^{\infty} \frac{\sin \omega_n t^*}{n^2 T_n}$$

Take the first mode by letting n = 1:

$$\lim_{t_1 \longrightarrow 0} \frac{R_D}{R_S} = \frac{8}{\pi} \frac{t_1}{T_1} \sin 2\pi \frac{t^*}{T_1} \qquad (12)$$

The foregoing derivation has shown that for the conditions of very short pulse duration (say when $t_1/T_1 < 1/3$) and constant impulse, the peak normalized reaction approaches a value equal to $(8/\pi)\, t_1/T_1$. A plot of reaction for $t > t_1$ in which the load pulse satisfies the two conditions should verify (12).

4. Dynamic Center Moment and Beam Resistance Parameter

The moment at any point x along the beam is given by:

$$M = - EI \frac{\partial^2 w}{\partial x^2}$$

Performing the differentiation on (9), evaluating at $x = \ell/2$ and noting that $P_m \ell^2/8$ is the maximum static center moment if P_m were applied as a static load:

$$\frac{M_D}{M_S} = \frac{32}{\pi^3} \sum_{n=\text{odd}}^{\infty} \frac{(-1)^{\frac{n-1}{2}}}{n^3} \left[\left(1 - \cos 2\pi n^2 \frac{t}{T_1} \right) \right.$$

$$\left. - 1/(t_1/T_1) \cdot t/T_1 \left(1 - \frac{\sin 2\pi n^2 \, t/T_1}{2\pi n^2 \, t/T_1} \right) \right] \qquad (13)$$

A plot of M_D/M_S versus the time parameter t/T_1 furnishes a convenient means of defining the limits of elastic and plastic beam action for different pulse durations. As in the reaction plots, the first mode ($n = 1$) in (13) is used as a good approximation. Given a curve of M_D/M_S versus t/T_1, the fully plastic moment of the beam cross-section may be considered to have been reached for different values of M_D. When a given M_D/M_S is said to equal M_P/M_S, the time corresponding to the particular value of M_D/M_S is the time of hinge formation, t_p. The beam resistance parameter, M_P/M_S may be thought of as the ratio of the yield value of the beam's moment resistance to the maximum moment caused by the static application of P_m.

III. PLASTIC BEHAVIOR OF WALL PANELS

A. Statement of the Problem

1. Assumptions in the Simplified Plastic Analysis

In order to derive a fairly simple expression for beam reaction when the beam ceases to behave elastically, the following assumptions are made:

a. A plastic hinge forms at the center of the beam when the dynamic center moment, M_D reaches a value equal to the fully plastic moment of the section, M_P. This time is designated t_p.

b. Neglect the elastic bending of the beam.

c. Assume that deflections are small.

d. Assume that M_D remains equal to M_P until the beam velocity becomes equal to zero. At this point, M_D becomes less than M_P, the center hinge disappears, and the beam behaves elastically again.

Figure 6 represents the idealized plastic behavior of the beam conforming to the above assumptions.

Figure 7 is a free body diagram of half of the beam from which equations of motion may be written as follows:

$$\sum F_w = M \ddot{\bar{w}} \quad \text{where } \bar{w} = \frac{\ell}{4}\theta;\ \ddot{\bar{w}} = \frac{\ell}{4}\ddot{\theta}$$

$$\frac{p\ell}{2} - R = \frac{m\ell}{2} \cdot \frac{\ell}{4}\ddot{\theta} \tag{14}$$

$$\sum T_o = I_o \ddot{\theta} \quad \text{where} \quad I_o = \frac{1}{3}\frac{m\ell}{2}\left(\frac{\ell}{2}\right)^2 = \frac{m\ell^3}{24}$$

$$\frac{p\ell}{2} \cdot \frac{\ell}{4} - M_P = \frac{m\ell^3}{24}\ddot{\theta} \tag{15}$$

B. Reaction Expression

From Equation (15) solve for the angular acceleration:

$$\ddot{\theta} = \frac{24}{m\ell^3}\left(\frac{p\ell^2}{8} - M_P\right) \tag{16}$$

Substitute (16) into Equation (14) and solve for R:

$$R = \frac{p\ell}{8} + \frac{3M_P}{\ell} \quad \text{where } p = \text{function of time.} \tag{17}$$

In Equation (17), p is the external load acting on the beam at time t' measured after the formation of the center hinge. Figure 8 represents the time origins for the different phases of beam action which occur during the load pulse.

With

$$p = p(t') = P_m\left[1 - \left(\frac{t' + t_p}{t_1}\right)\right]$$

and $t' = t - t_p$, and noting again that $P_m\ell/2$ is the maximum static reaction:

$$\frac{R_D}{R_S} = \frac{1}{4}\left[1 - 1/(t_1/T_1)\left(\frac{t' + t_p}{T_1}\right) + \frac{24M_P}{P_m\ell^2}\right] \tag{18}$$

Differentiation of (18) with respect to the time parameter, t'/T_1 gives the result that the slope, S, of the plastic reaction curve depends only on the pulse duration, or:

$$S = -\frac{1}{4}\ 1/(t_1/T_1) = -\frac{K}{4} \quad \text{if} \quad K = 1/(t_1 T_1) \tag{19}$$

C. Duration of Plastic Behavior

1. Expression for t_e

As stated in the assumptions for the plastic analysis, the center hinge disappears when the beam velocity becomes equal to zero. The time, t_e, at which the beam stops moving down is therefore the end of the plastic phase and the beginning of the elastic recovery phase.

In order to find t_e, an expression for the angular velocity of the beam can be derived which holds during the plastic phase ($t_p < t \leq t_e$). Equating this angular velocity to zero and solving for the time will yield the equation for t_e.

Differentiating Equation (9) with respect to time and evaluating at $x = \ell/2$ gives the linear velocity of the beam center, $\dot{w}_c$ during the initial elastic phase. For small deflections, the average angular velocity of half of the beam would be $= 2/\ell\ \dot{w}_c$. Performing these operations and setting $t = t_p$ will give the equation for the initial angular velocity at $t' = 0$ ($t = t_p$). (Figure 8) Thus:

$$\dot{\theta}'_o = \frac{8P_m \ell^3}{\pi^5 EI} \sum_{n=\text{odd}}^{\infty} \frac{(-1)^{\frac{n-1}{2}}}{n^5} \left[\omega_n \sin \omega_n t_p - \frac{1}{t_1} (1 - \cos \omega_n t_p) \right] \tag{20}$$

The required angular velocity may now be found by integrating (16) which was derived from the equations of motion for the plastic phase.

Noting that p in (16) =

$$p(t') = P_m \left[1 - \left(\frac{t' + t_p}{t_1} \right) \right] \quad :$$

$$\ddot{\theta}' = \frac{3P_m}{m\ell} \left[\left(1 - \frac{t' + t_p}{t_1} \right) - \frac{8M_P}{P_m \ell^2} \right]$$

Integrating and evaluating the constant of integration by using (20):

$$\dot{\theta}' = \frac{3P_m}{m\ell} \left\{ t' \left[1 - \frac{1}{t_1} \left(\frac{t'}{2} + t_p \right) - \frac{M_P}{M_S} \right] \right.$$

$$\left. + \frac{8m\ell^4}{3\pi^5 EI} \sum_{n=\text{odd}}^{\infty} \frac{(-1)^{\frac{n-1}{2}}}{n^5} \left[\omega_n \sin \omega_n t_p - \frac{1}{t_1} \left(1 - \cos \omega_n t_p \right) \right] \right\}$$

Simplify by letting n = 1 (first mode) and note that $\omega_1^2 = \pi^4 EI/m\ell^4$:

$$\dot{\theta}' = \frac{3P_m}{m\ell} \left\{ t' \left[1 - \frac{1}{t_1} \left(\frac{t'}{2} + t_p \right) - \frac{M_P}{M_S} \right] \right.$$

$$\left. + \frac{8}{3\pi\omega_1} \left[\sin \omega_1 t_p - \frac{1}{\omega_1 t_1} \left(1 - \cos \omega_1 t_p \right) \right] \right\} \qquad (21)$$

When (21) is equated to zero, the resulting equation is a quadratic in t' which can be solved by the quadratic formula giving the following result when put in dimensionless form:

$$\frac{t_e}{T_1} = \frac{t_p}{T_1} + \left\{ - \frac{t_1}{T_1}\left(\frac{M_P}{M_S} + \frac{1}{\frac{t_1}{T_1}}\,\frac{t_p}{T_1} - 1\right) + \sqrt{\left[\frac{t_1}{T_1}\left(\frac{M_P}{M_S} + \frac{1}{\frac{t_1}{T_1}}\,\frac{t_p}{T_1} - 1\right)\right]^2 + \frac{8}{3\pi^2}\,\frac{t_1}{T_1}\left[\sin\frac{2\pi t_p}{T_1} - \frac{1}{2\pi\,\frac{t_1}{T_1}}\left(1 - \cos\frac{2\pi t_p}{T_1}\right)\right]}\right\} \quad (22)$$

IV. ELASTIC RECOVERY PHASE OF WALL PANEL BEHAVIOR

A. Statement of the Problem

1. Application of Dynamic Beam Equation

Equation (22) defines the time at which the beam again behaves elastically. The derivation of this elastic recovery reaction expression follows the same method as used on the initial one; however, one free vibration term is added. When $t'' = 0$ $(t = t_e)$, the initial velocity, $\dot{w}_o''$ of the beam is zero, but the initial displacement, w_o'' has a finite value. An examination of the formulae for A_n and B_n (Section II) shows that the first free vibration term in Equation (7) has a value other than zero.

For time measured from t_e ($t'' = t - t_e$), the elastic deflection is still of the form:

$$w''(x) = \sum_{n}^{\infty} X_n \tau_n$$

where $X_n = \sin n\pi x/\ell$ and

$$\tau_n = A_n \cos \omega_n t'' + \frac{P_n}{m\omega_n} \left[\sin \omega_n t'' \int_o^{t''} \varphi(t'') \cos \omega_n t'' dt'' \right.$$

$$\left. - \cos \omega_n t'' \int_o^{t''} \varphi(t'') \sin \omega_n t'' dt'' \right] \qquad (23)$$

where $P_n = 4/n\pi$ when n = odd. (See Equation (2).)

The constant A_n is defined as

$$A_n = \frac{\int_o^{\ell} w_o''(x)\, X_n\, dx}{\int_o^{\ell} X_n^2\, dx} = \frac{2}{\ell} \int_o^{\ell} w_o''(x)\, X_n\, dx \qquad (24)$$

Now let $w_o''(x) = \overline{w}_{c_e} \sin \frac{\pi x}{\ell}$ where $\overline{w}_{c_e}$ is the effective center deflection at the beginning of the elastic recovery phase. At first glance it appears that a good approximation of $w_o''(x)$ should be given by

$$w_o''(x) = w_{c_m} \sin \frac{\pi x}{\ell}$$

where w_{c_m} is the center deflection of the beam in the plastic phase at the instant the beam reaches its maximum deflection in the positive

direction (in direction of applied load) and begins to rebound elastically. However, it is apparent that the maximum amplitude of the elastic center deflection is much less than the corresponding maximum amplitude of the plastic center deflection. Figure 9 illustrates roughly this difference. The solid curve gives an idea of the actual variation of reaction with center deflection throughout the two elastic phases and the single plastic phase. The dotted curve is an approximation to the actual behavior which suggests a simple means of obtaining a close estimate of $\overline{w}_{c_e}$. As shown in the figure, the maximum plastic center deflection, w_{c_m} is much greater than $\overline{w}_{c_e}$; and w_y, the center deflection at the time of hinge formation (t_p) is approximately equal to $\overline{w}_{c_e}$.

The final expression and best approximation to be used for $w_o''(x)$ is thus:

$$w_o''(x) = w_y \sin \frac{\pi x}{\ell}$$

The value of w_y may be found from Equation (9) by setting $x = \ell/2$ and $t = t_p$. The result is:

$$w_y = \frac{4P_m \ell^4}{\pi^5 EI} \sum_{n=\text{odd}}^{\infty} \frac{(-1)^{\frac{n-1}{2}}}{n^5} \left[(1 - \cos \omega_n t_p) - \frac{t_p}{t_1} \left(1 - \frac{\sin \omega_n t_p}{\omega_n t_p} \right) \right] \quad (25)$$

For simplicity, equate all the values of A_n to zero except A_1. The value of A_1 may then be found by setting $n = 1$ in $X_n = \sin \frac{n\pi x}{\ell}$. (24) A_1 is then given by:

$$A_1 = \frac{2}{\ell} \int_o^{\ell} w_y \sin^2 \frac{\pi x}{\ell} \, dx = w_y$$

The expression for A_1 is thus identical to w_y. (25)

Substituting the value of $\varphi(t'')$ (Figure 8) in (23) and performing the integrations leads to values of τ_n as follows:

$$\tau_1 = A_1 \cos \omega_1 t'' + \frac{4P_m}{(1)\pi m\omega_1^2} \left\{ - \cos \omega_1 t'' \left(1 - \frac{t_e}{t_1}\right) + \frac{\sin \omega_1 t''}{\omega_1 t_1} + \left[1 - \left(\frac{t'' + t_e}{t_1}\right)\right]\right.$$

$$\tau_3 = 0 + \frac{4P_m}{(3)\pi m\omega_3^2} \left\{ - \cos \omega_3 t'' \left(1 - \frac{t_e}{t_1}\right) + \frac{\sin \omega_3 t''}{\omega_3 t_1} + \left[1 - \left(\frac{t'' + t_e}{t_1}\right)\right]\right.$$

The remaining τ_n terms are formed in a similar manner.

B. Reaction Expression

The basic expression for deflection (page 20) may now be used directly to obtain the beam end reaction:

$$R_D = EI \frac{\pi^3}{\ell^3} \sum_{n=\text{odd}}^{\infty} n^3 \tau_n \qquad (26)$$

An approximate equation for R_D is obtained by ignoring all τ_n in (26) for $n > 1$ and taking only one term in the summation of (25). In dimensionless form for plotting, the approximate reaction expression for $t_e < t < t_1$ is:

$$\frac{R_D}{R_S} = \frac{8}{\pi^2} \left\{ \cos 2\pi \frac{t''}{T_1} \left[\left(1 - \cos 2\pi \frac{t_p}{T_1}\right) - \frac{1}{t_1/T_1} \cdot \frac{t_p}{T_1} \left(1 - \frac{\sin 2\pi\, t_p/T_1}{2\pi\, t_p/T_1}\right) \right.\right.$$

$$\left. - \left(1 - \frac{1}{t_1/T_1} \cdot \frac{t_e}{T_1}\right)\right] + \frac{\sin 2\pi\, t''/T_1}{2\pi\, t_1/T_1} + \left.\left[1 - \frac{1}{t_1/T_1}\left(\frac{t'' + t_e}{T_1}\right)\right]\right\} \qquad (27)$$

V. RESULTS AND DISCUSSION

A. Frame Load Charts

1. Construction of Charts

In the previous sections of this paper, expressions for the beam end reactions have been derived for the elastic and plastic phases of beam behavior. The reaction is expressed as a ratio of the dynamic end reaction to the maximum static end reaction, (R_D/R_S); the time parameter is written as the ratio of the elapsed time to the fundamental natural period of the beam (t/T_1); and the beam resistance parameter is expressed as the ratio of the fully plastic moment of the section to the maximum static center moment (M_P/M_S). For convenience, the following table lists the various phases of beam action, the time range of each phase (Figure 8), and the governing reaction equation:

Phase	Time Range	Equation
Initial Elastic	$0 < t < t_p$	(10)
Plastic	$t_p < t < t_e$	(18)
Elastic Recovery	$t_e < t < t_1$	(27)

Figures 23, 27, and 29 contain plots of all three phases. The remaining reaction curves include only the initial elastic and the plastic phases. On the same graph with each reaction plot is shown the external load which impinges on half the beam. Thus at $t = 0$, the load on half the beam is $P_m \ell/2$; the maximum static end reaction is also $P_m \ell/2$; therefore the initial ratio of the half-beam load to the maximum static reaction is equal to one. The external load line thus starts at unity at $t = 0$, and drops in a

straight line to zero at $t = t_1$. This is, then, a graphical representation of the load which arrives on half of the beam, and what this half beam transmits on to the frame as end reaction.

The moment curves are used to find the value of t_p for a given pulse duration t_1, and resistance parameter (M_P/M_S). (Figure 16) The duration of the initial elastic phase is thus determined graphically from the plot of M_D/M_S versus t/T_1 by allowing M_D to equal M_P as M_P changes over a range of values. This brings in the shape and physical characteristics of the beam since the fully plastic moment varies with the shape and material.

The duration of the plastic phase is fixed by Equation (22). The loci of these times as found by solving (22) form a smooth curve and are plotted on the reaction graphs. It will be noted that for a given pulse duration, the loci of Equation (22) indicate the expected results; that is, that beams of low resistance (small M_P/M_S) have long plastic phases and vice versa.

In the construction of the reaction curves, it was found that a discontinuity always existed between the elastic and plastic phases. This "jump" in reaction value is due to the relatively rough assumptions of the plastic analysis used, the main error being the neglect of elastic bending of the beam. Since the source of the discontinuity was known, the reaction values were corrected by the amount of the initial reaction error.

Plots of the elastic recovery phase were made only for a few representative values of t_1/T_1 and M_P/M_S as follows:

	t_1/T_1	M_P/M_S	Fig.
a. As an example of a short pulse	0.8	1.0	23
b. As examples of long pulses	5.0	1.4	27
	5.0	1.0	27
	10.0	1.4	29
	10.0	1.0	29

2. Comparison of First Mode and More Exact Reaction Curves[6]

As stated in the introductory statement, no attempt is made in this study to find out by analytical procedures the accuracy with which the first mode approximation represents the exact elastic reaction curve. However, for the initial elastic phase, Equation (10) was expanded and data was collected to plot curves for one term (n = 1), three terms (n = 1, 3 and 5), and 6 terms (n = 1, 3, 5, 7, 9 and 11) in order that a graphical comparison could be made.

Figure 11 shows the results of the plot for a very short pulse. It is obvious that the first mode approximation is not good for load pulses of such short duration. Figure 35 illustrates the very great improvement in the accuracy of the first mode approximation for pulses of very long duration. It would seem reasonable to expect then, that as the load pulse duration increases

[6] This subsection refers to the uncompensated first mode reaction curves as derived from Equation (10) by setting n = 1. These curves are indicated in Figures 11, 19 and 35. As brought out in the following subsection, all other reaction plots are constructed using the first mode multiplied by a compensating factor.

from a small to a large value, the accuracy of the first mode should show a gradual improvement. Figure 19 furnishes evidence of this trend since it shows the first mode curve to be a better approximation than it is for $t_1/T_1 = 0.1$ but not as good as for $t_1/T_1 = 100.0$.

One situation in which the first mode curve gives a false impression is encountered at very small values to t/T_1 and M_P/M_S. An example is Figure 11. Here the reaction in the plastic phase for $M_P/M_S = .05$ appears to become negative before the end of the pulse. It is apparent, however, that negative values would not be indicated if the plastic phase plot were started from the more exact initial elastic curve (for 3 or 6 terms). An examination of pulses of longer duration will indicate this same ambiguity at very small values of t/T_1 and M_P/M_S.

3. Method Used to Make First Mode Approximation More Conservative

Figures 11, 19, and 35 show that the first mode reactions plotted from Equation (10) generally furnish values lower than those indicated by the more exact curves. In order to retain the advantages of the first mode approximation but at the same time to obtain more conservative end reaction magnitudes, the reaction expressions for the two elastic phases (Equations (10) and (27) with n = 1) were multiplied by a factor of $\pi^2/8$. This step also increased the plastic reaction values by the same factor since the plastic phase merges with the two elastic phases. The reasoning behind the use of this factor follows.

The use of the first mode curves for elastic reaction neglects the contribution of the higher modes in (10) and (27) to the end reaction.

Such a simplifying approximation may be considered as being equivalent to using an instantaneous beam loading represented by the first term in the Fourier Series expansion of a uniform load. This first term in the Fourier expansion is merely a simple sine curve distribution of load. Therefore, the actual pressure load which at any instant is uniformly distributed, is replaced by a sine curve loading the total magnitude of which is very close to that of the actual load. Figure 36 illustrates the shapes of the actual and approximately-equivalent loadings.

The ratio of the end reaction calculated from the correct loading to that derived from the equivalent sine curve loading is found as follows: (Figure 36)

$$R_{(1)} = \frac{p(t)\ell}{2}$$

$$R_{(2)} = \frac{1}{2} \int_0^{\ell} \frac{4}{\pi}\ p(t) \sin \frac{\pi x}{\ell}\, dx = \frac{4p(t)\ell}{\pi^2}$$

then

$$\frac{R_{(1)}}{R_{(2)}} = \frac{\pi^2}{8}$$

It seems reasonable then, that reaction values more nearly equal to those resulting from a uniform load will result if Equations (10) and (27) (setting n = 1) are multiplied by the factor $\pi^2/8$. Such a procedure was followed in this paper.

Figures 11, 19 and 35 contain plots of the initial elastic reaction expression wherein a comparison is made of the curves plotted from Equation (10) for the following conditions:

(1) n = 1

(2) n = 1 using multiplication factor of $\pi^2/8$

(3) three terms (n = 1, 3, 5)

(4) six terms (n = 1, 3, 5, 7, 9, 11)

This graphical comparison shows that the use of the first mode multiplied by the factor $\pi^2/8$ gives results which are more conservative approximations to the more exact curves.

Since values of t_p/T_1 are determined graphically from the M_D/M_S versus t/T_1 plot, another source of error in the first mode reaction curves is the use of only the first term (n = 1) in Equation (13). However, the elastic center moment varies as $\frac{1}{n^3}$ for n equal to odd integers; therefore, the approximation for center moment is less in error than the corresponding approximation for reaction since elastic reaction varies as $\frac{1}{n^2}$. A comparison of the center moments due to the two loadings in Figure 36 gives the following result:

$$M_{(1)} = \frac{p(t)\ell^2}{8} = 0.125\ p(t)\ell^2$$

$$M_{(2)} = \frac{4p(t)\ell^2}{\pi^2}\ (.500 - .182) = 0.129\ p(t)\ell^2$$

then

$$\frac{M_{(1)}}{M_{(2)}} = \frac{.125}{.129} = \frac{1}{1.032} = .970$$

By the foregoing reasoning, more accurate values of t_p/T_1 could be gained by multiplying Equation (13) by 0.970. This factor is so close to unity, however, that little change in the values of t_p/T_1 would result. In this study, Equation (13) with n = 1 was used as derived without applying the correction factor.

4. Discussion of Different Phases of Wall Panel Action

In the introduction to this paper, the statement was made that the characteristics of the wall panels would cause the shape of the load transmitted to the frame to be much different from that which impinges on the panels themselves. A study of the Frame Load Charts (end reaction curves) bears out this statement. The wall panels are acted upon by an initial-peak, triangular loading pulse but send to the frame by means of the end reactions, a loading which has been radically altered in shape.

The unit load which reaches the supporting members rises gradually from zero along the initial elastic reaction curve. Depending on the duration of the blast pulse and the beam resistance parameter, the beam (wall panel) becomes plastic at a certain time and the reaction then decreases linearly with time at a rate depending only on the pulse duration. Then if the panel has sufficient elastic resistance, the action again becomes elastic and remains so throughout the remainder of the load pulse.

For very short pulse durations, the plastic phase continues to the end of the pulse and no elastic recovery phase occurs. Figures 11, 13, and 15 illustrate this behavior. As the pulse durations increase, the elastic recovery phase begins to appear starting with panels of high elastic resistance (large M_p/M_s). Figures 27 and 29 show how (for long

pulse durations) the two elastic reaction curves oscillate about the incident load line. It should be noted here that damping will tend to decrease the amplitude of the elastic oscillations about the load line. If the effects of damping could have been included in the derivations of the elastic reaction expressions, Figures 27 and 29 would probably indicate a gradual decrease with time in the amplitude of the vibrations of elastic reaction about the external load line. Thus, in the elastic recovery phase for low beam resistances, the elastic reaction would become coincident with the load line as t approaches t_1.

Theoretically, if a wall panel had infinite elastic resistance, its end reaction would follow the initial elastic curve and the frame loads would rise to a maximum. Plastic action takes place however, since the panels have finite elastic resistance, and prevents the frame loads from building up to these peak values. The formation of the center plastic hinge, thus effectively cuts off the top of the elastic reaction curve and consequently permits smaller loads to reach the frame.

The occurrence of negative values of reaction in the elastic oscillations about the load line may be highly significant under certain conditions. If the fasteners used to attach the wall panels to the supporting frame are not designed to withstand tension loads, it is very possible that such fasteners will fail at the time the wall panel end reaction first becomes negative. Such failure would alter the frame loads in the case of load pulses of sufficient duration ($t_1/T_1 > 0.8$ in the frame load charts), limiting the loads transmitted by the panels tc the supporting members to a single positive pulse.

B. Tables and Graphs of Results

Table 1 is presented for convenient reference. For given values of pulse duration (t_1/T_1), plots are also made of the beam resistance parameter (M_p/M_s) versus both the duration of the initial elastic phase (t_p/T_1) and the duration of the plastic phase ($t_e/T_1 - t_p/T_1$). (Figures 37 and 39) Similar graphs are drawn with M_p/M_s as the fixed parameter. (Figures 38 and 40)

Figure 37 shows that the duration of the initial elastic phase increases almost linearly with increasing values of M_p/M_s for fixed load durations. Figure 38 demonstrates that for a given beam resistance, the duration of the load pulse has little effect on the length of time which the panel remains elastic except in the case of the shorter load pulses.

As might be expected, there is a very great increase in the duration of the plastic phase (for given pulse duration) with a decrease in wall panel resistance. (Figure 39) The increase is most pronounced for long load pulse durations.

Figure 40 shows that the effect of load duration is largest for low values of panel resistance, and that, in general, the plastic phase duration decreases as the duration of the load decreases (with given panel resistance).

Table 1

t_1/T_1		Values of M_P/M_S											
		.05	0.1	0.2	0.4	0.6	0.8	1.0	1.2	1.4	1.6	1.8	2.0
	1**			.100	.146	.182	.214	.244	.276	.308	.343	.385	.448
100.0	2**			*	*	80.100	40.430	5.190	.922	.631	.529	.496	.492
	1			.100	.146	.182	.214	.245	.276	.309	.344	.385	.448
50.0	2			*	*	40.100	20.400	3.571	.903	.616	.527	.494	.490
	1			.100	.146	.182	.215	.246	.277	.310	.345	.388	.455
20.0	2			*	*	16.132	8.415	2.325	.855	.604	.522	.492	.490
	1			.100	.146	.182	.216	.247	.278	.311	.348	.392	.470
10.0	2			*	*	8.122	4.396	1.649	.792	.586	.514	.488	.490
	1			.102	.146	.184	.216	.248	.280	.314	.352	.398	
5.0	2			*	*	4.123	2.378	1.170	.707	.557	.500	.480	
	1			.104	.150	.188	.224	.262	.300	.348	.450		
1.0	2			*	*	.918	.681	.540	.472	.444	.450		
	1			.104	.150	.192	.228	.258	.310	.368			
0.8	2			*	*	.756	.586	.486	.443	.430			
	1			.105	.155	.195	.235	.275	.330				
0.6	2			*	*	.595	.488	.432	.410				
	1			.104	.154	.196	.240	.288	.360				
0.5	2			*	*	*	.438	.401	.396				
	1			.106	.158	.204	.250	.312					
0.4	2			*	*	*	.386	.372					
	1			.108	.162	.216	.280						
0.3	2			*	*	*	*						
	1		.076	.112	.178	-	-						
0.2	2		*	*	*								
	1	.055	.084	-	-								
0.1	2	*	*										

*Beam velocity does not reach zero during time of pulse

1** t_p/T_1

2** t_e/T_1

C. Frame Loads After Termination of Load Pulse

For time beyond the end of the pulse, the derivation of the elastic reaction expression is similar in procedure to that used in Section II in finding the limiting reaction for short pulses and constant load impulse. Equation (26) would be used to find the displacement and velocity at $t = t_1$ in order that A_n and B_n could be evaluated; the expression for w would then be found where

$$w = \sum_{n}^{\infty} X_n \tau_n$$

and X_n still equals $\sin n\pi x/\ell$. Reaction could be found as before by evaluating the shear at $x = 0$.

VI. SUMMARY AND CONCLUSIONS

A. Applications of Frame Load Charts

A method has been found for determining the load-time relation for blast load transmitted by the wall panels of a structure to the supporting members. The frame load charts may be used for three possible types of wall panel behavior; a purely elastic action, an elasto-plastic action, and a brittle action.

For a given pulse duration, and purely elastic behavior, the initial elastic phase reaction curves apply throughout the duration of the pulse. This assumes, of course, that the wall panel has sufficient elastic resistance (high M_P/M_S) to behave in this manner.

A more usual wall panel behavior is the elasto-plastic type. Here the elastic resistance is not high enough to confine the action to a purely elastic one. Given the pulse duration and beam resistance parameter, the frame load charts used in conjunction with the dynamic center moment curves indicate the loads which are transmitted by the wall panels to the frame.

Wall panels constructed of brittle material will behave elastically up to the ultimate moment carrying capacity of the panel (M_U) and then fracture suddenly. The time of fracture could be determined from the dynamic center moment curves by setting $M_D = M_U$ over a range of values of M_U. The frame load charts would indicate a rise in load along the initial elastic curve up to the point of fracture at which time the reaction would drop to zero.

In order to use the frame load charts for all three types of wall panel behavior, the following information must be available:

a. Wall panel span and a curve of side-on overpressure versus time from which P_m, t_1, R_S, and M_S, can be calculated.(7)

b. Dimensions and properties of wall panel in order that T_1, M_P and M_U may be calculated or estimated.

Entering the charts with t_1/T_1 and M_P/M_S or M_U/M_S, the magnitude and time distribution of the uniform frame load can be determined.

B. Conclusions

The frame load charts presented in this study represent an attempt to evaluate the loads received by the supporting members from the building covering when the walls are subjected to a blast pressure wave. Rough assumptions had to be made in some cases in order to obtain fairly simple expressions from which the load charts could be constructed. Also, since the elastic reaction expressions involve the sum of an infinite series of terms, they could not be used in their exact form. Therefore, the first mode approximations to the exact elastic reaction expressions were modified by a compensating factor of $\pi^2/8$ and then used to construct the frame load charts. It is felt that this step, although not theoretically exact, provides good engineering approximations to the actual blast loads which a frame would experience. Also, keeping in mind the

(7) N. M. Newmark, "An Engineering Approach to Blast Resistant Design", Proceedings ASCE, Vol. 79, Separate No. 306, October 1953.

additional condition that uncertainties in loading and in the structural properties of the wall panels will always exist, the author feels that the frame loads indicated by the charts are sufficiently accurate to be used in the design of building frames.

The basic relations for panel end reaction in all phases of elastic and plastic action which occur during the load pulse have been derived. For the values of pulse duration and beam resistance parameters considered, the load charts are complete through the initial elastic and plastic phases of wall panel action, and representative curves for the elastic recovery phase have been drawn. Thus the main purpose of the study -- that of determining the shape of the loads transmitted to the frame -- has been accomplished. Additional work is required to finish the elastic recovery phase and to extend the study to time beyond the end of the pulse using the methods outlined in this paper.

BIBLIOGRAPHY

1. N. M. Newmark, "An Engineering Approach to Blast Resistant Design", Proceedings ASCE, Vol. 79, Separate No. 306, October 1953.

2. S. Timoshenko, "Vibration Problems in Engineering", D. Van Nostrand Co., Inc., New York, N. Y., Second Edition, July 1937.

3. E. Jahnke and F. Emde, "Tables of Functions with Formulae and Curves", Dover Publications, New York, N. Y., Fourth Edition, 1943.

4. L. E. Goodman, "Behavior of Structures Under Dynamic Loads", Lecture Course in Structural Engineering, University of Illinois, 1953.

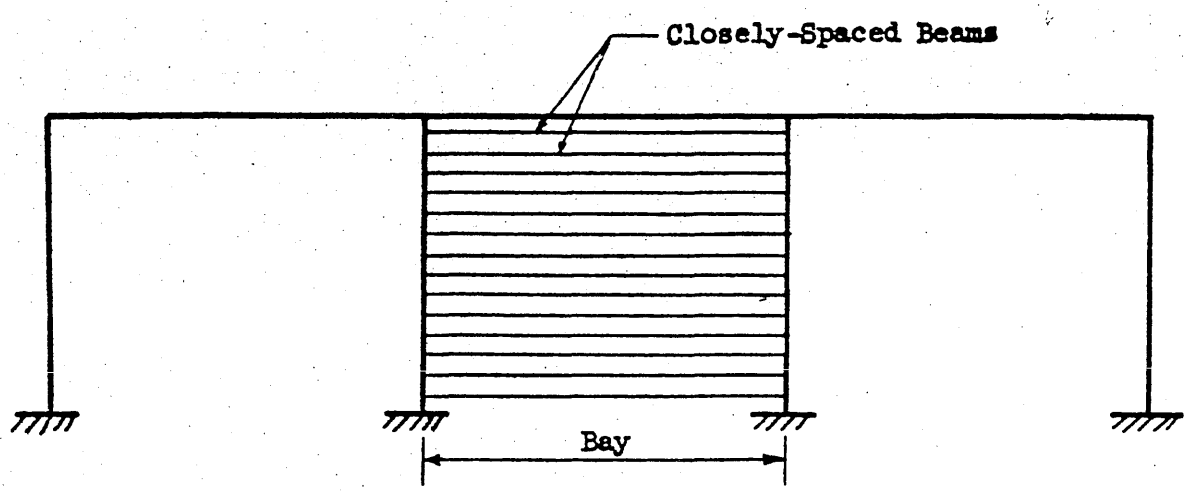

Figure 1- Typical Bay with Nest of Beams Approximating Wall Covering

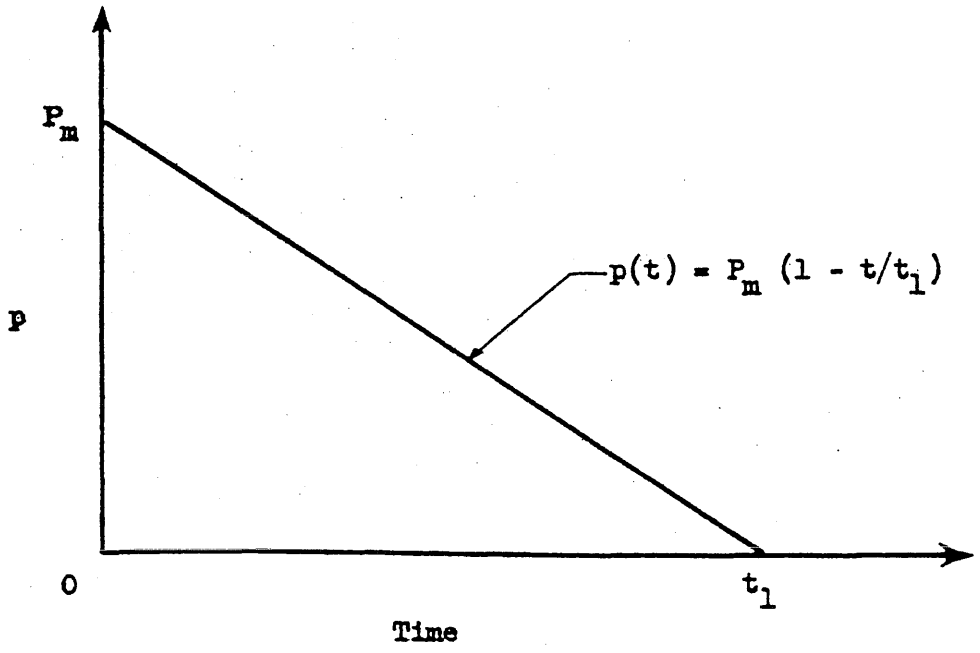

Figure 2- Triangular Load Pulse

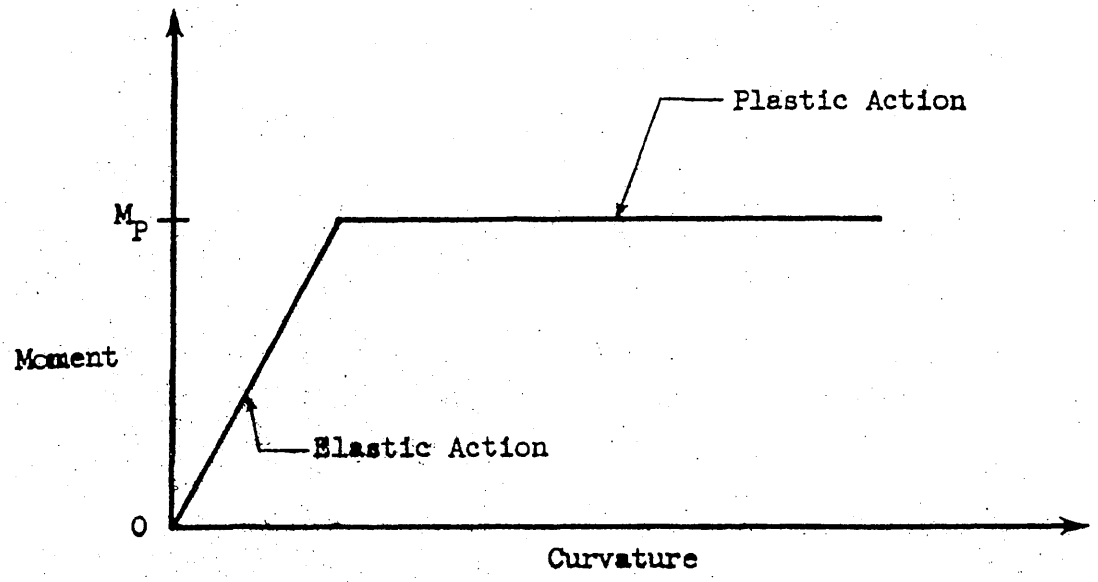

Figure 3— Idealized Elasto-Plastic Moment-Curvature Relation

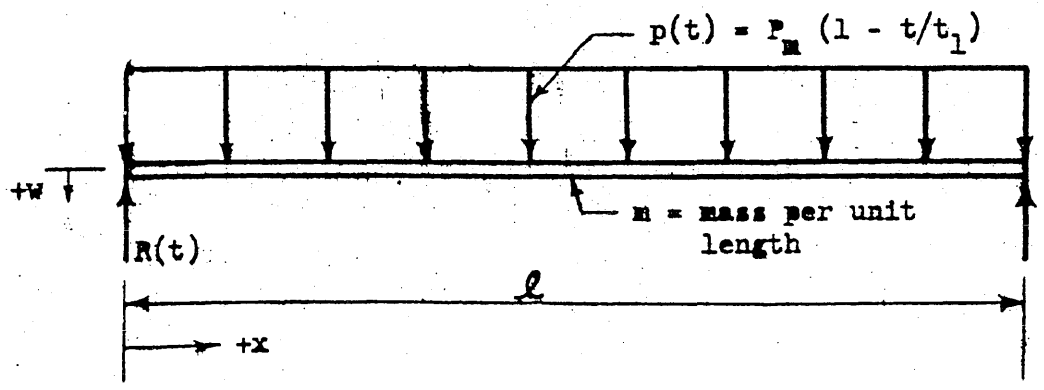

Figure 4— Typical Beam with Loading

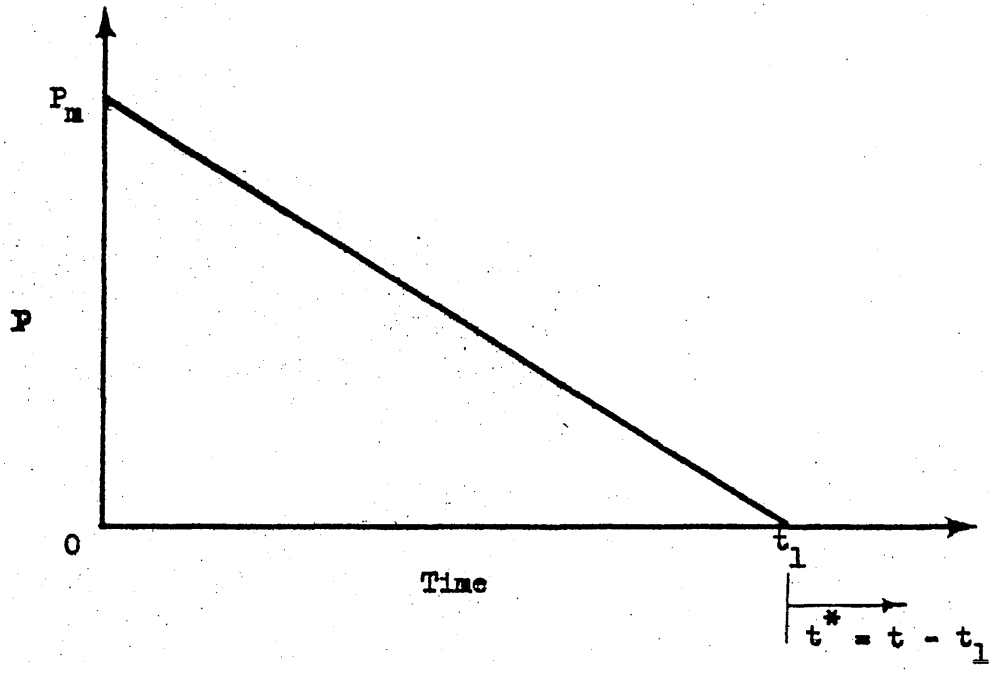

Figure 5- New Time Origin for $t > t_1$

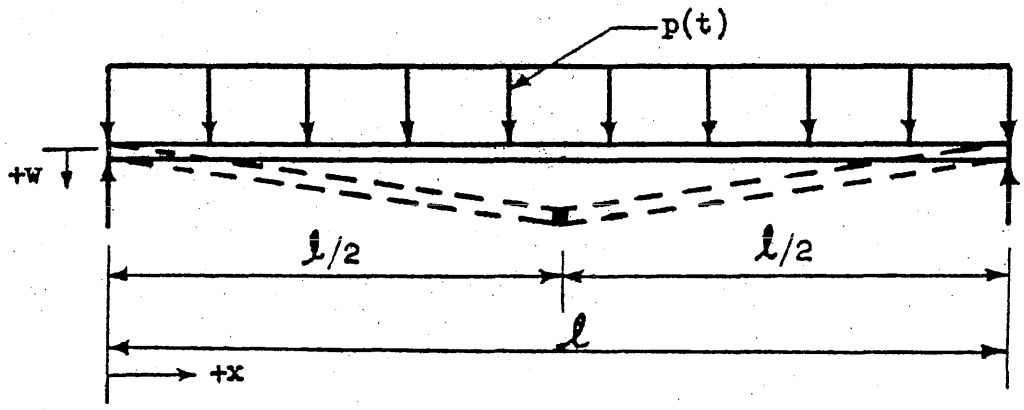

Figure 6 - Plastic Behavior of Beam

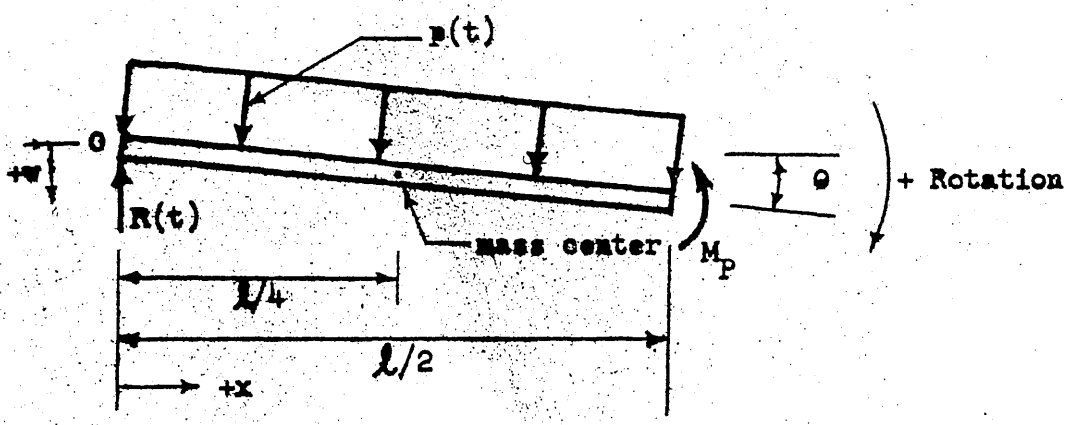

Figure 7 - Free Body Diagram of Plastic Beam

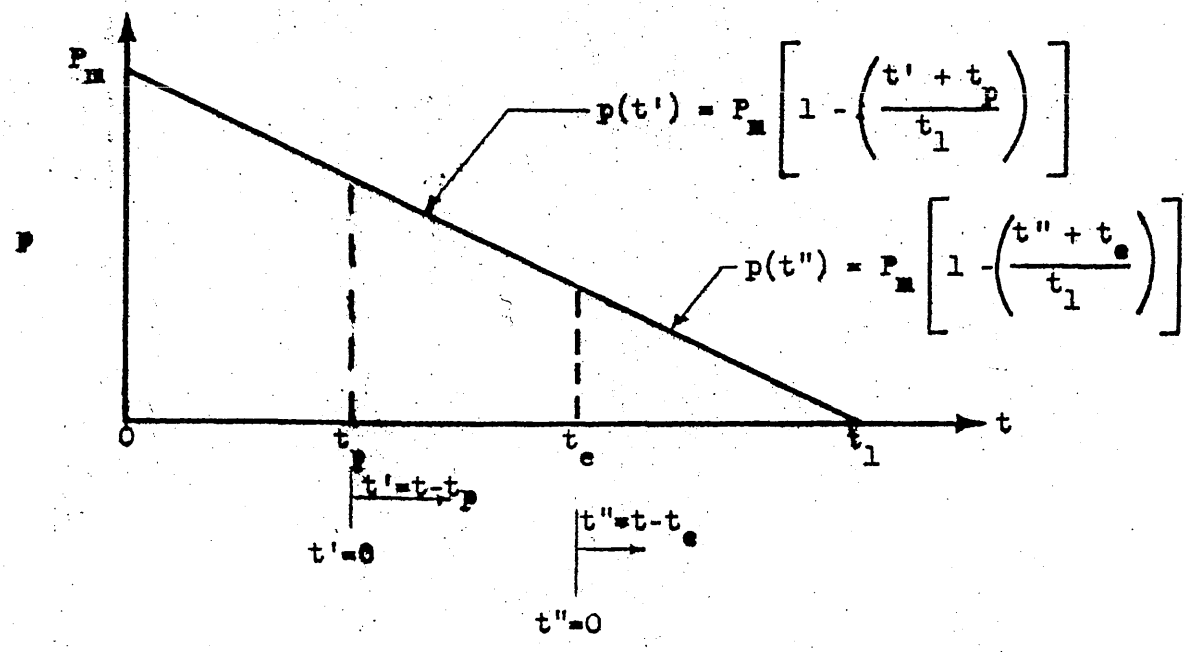

Figure 8 - Time Origins for Elastic and Plastic Phases

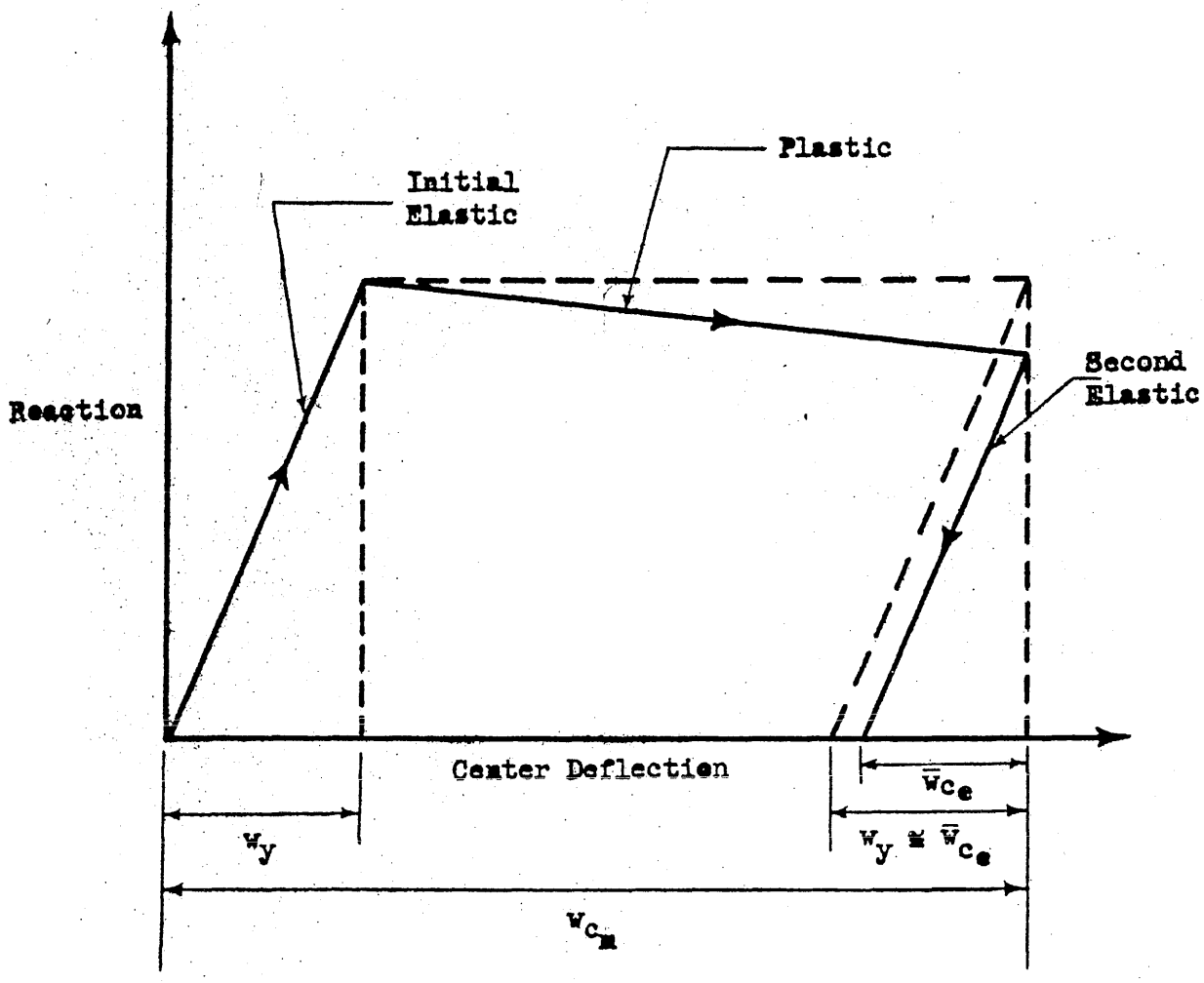

Figure 9 - Graphical Representation of Actual and Approximate Variation of End Reaction with Center Deflection

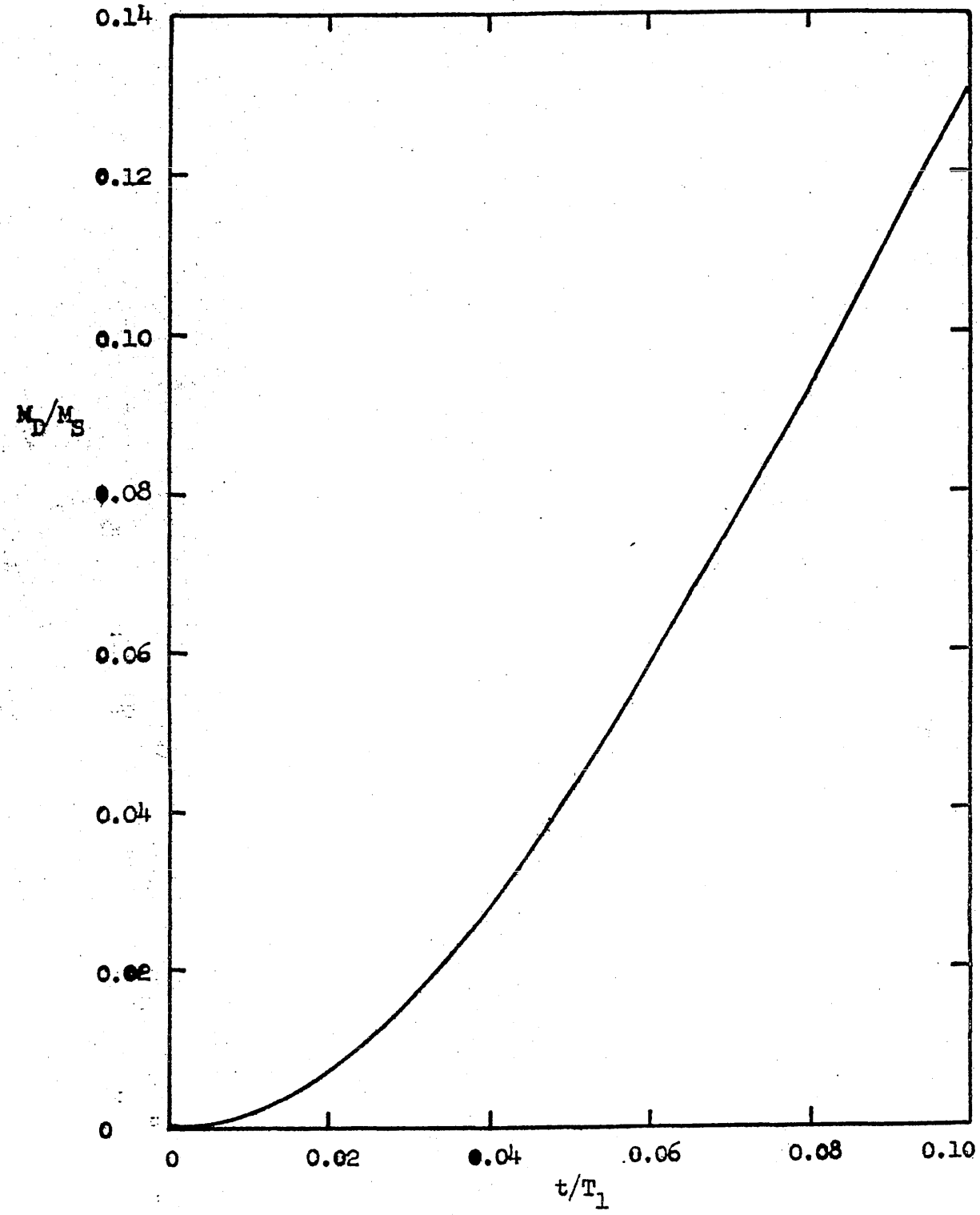

Figure 16 - Ratio of Dynamic Center Moment to Maximum Static Center Moment Versus Time Parameter (t_1/T_1 = 0.1)

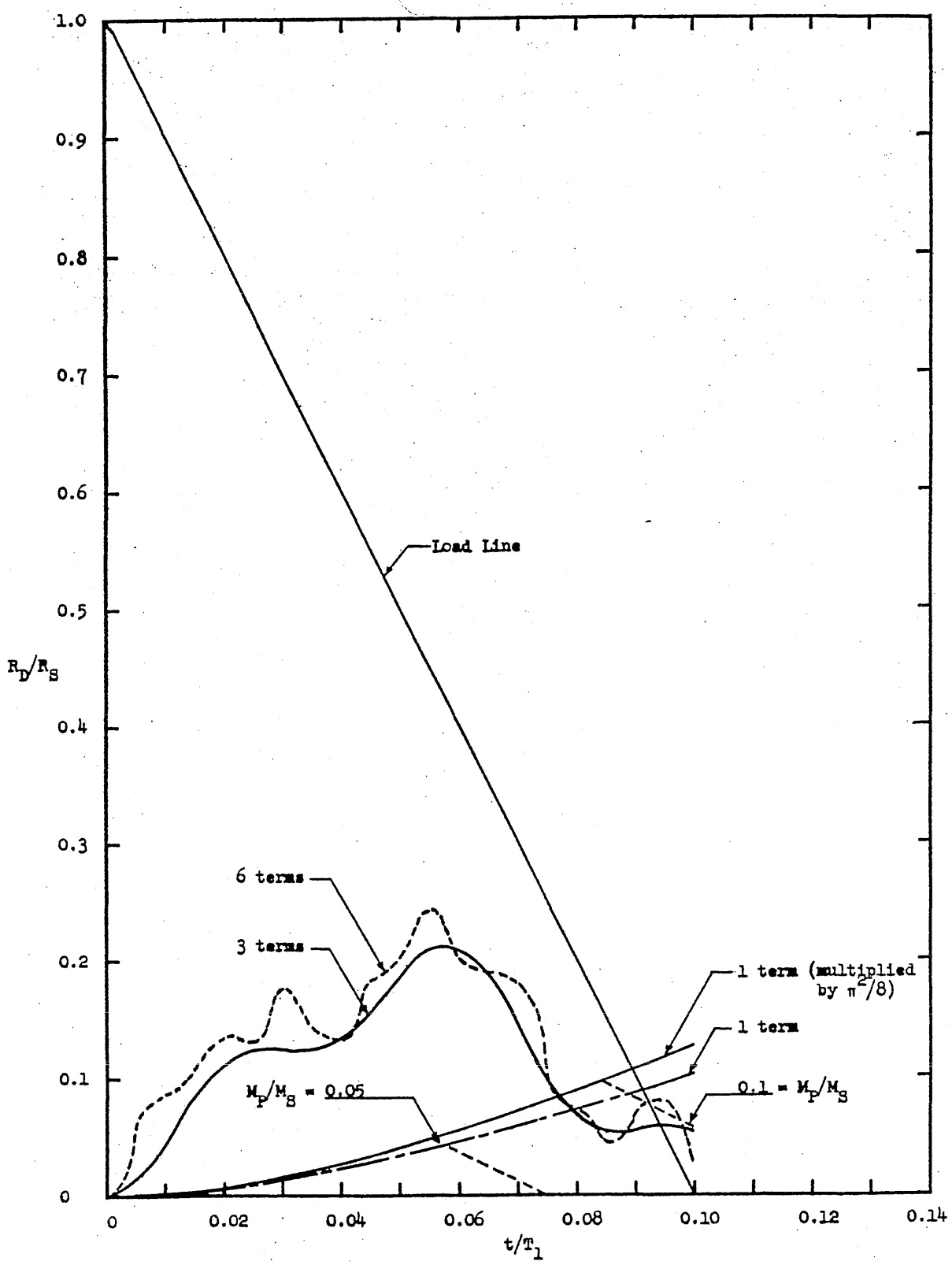

Figure 11 - Ratio of Dynamic End Reaction to Maximum Static End Reaction Versus Time Parameter (t_1/T_1 = 0.1)

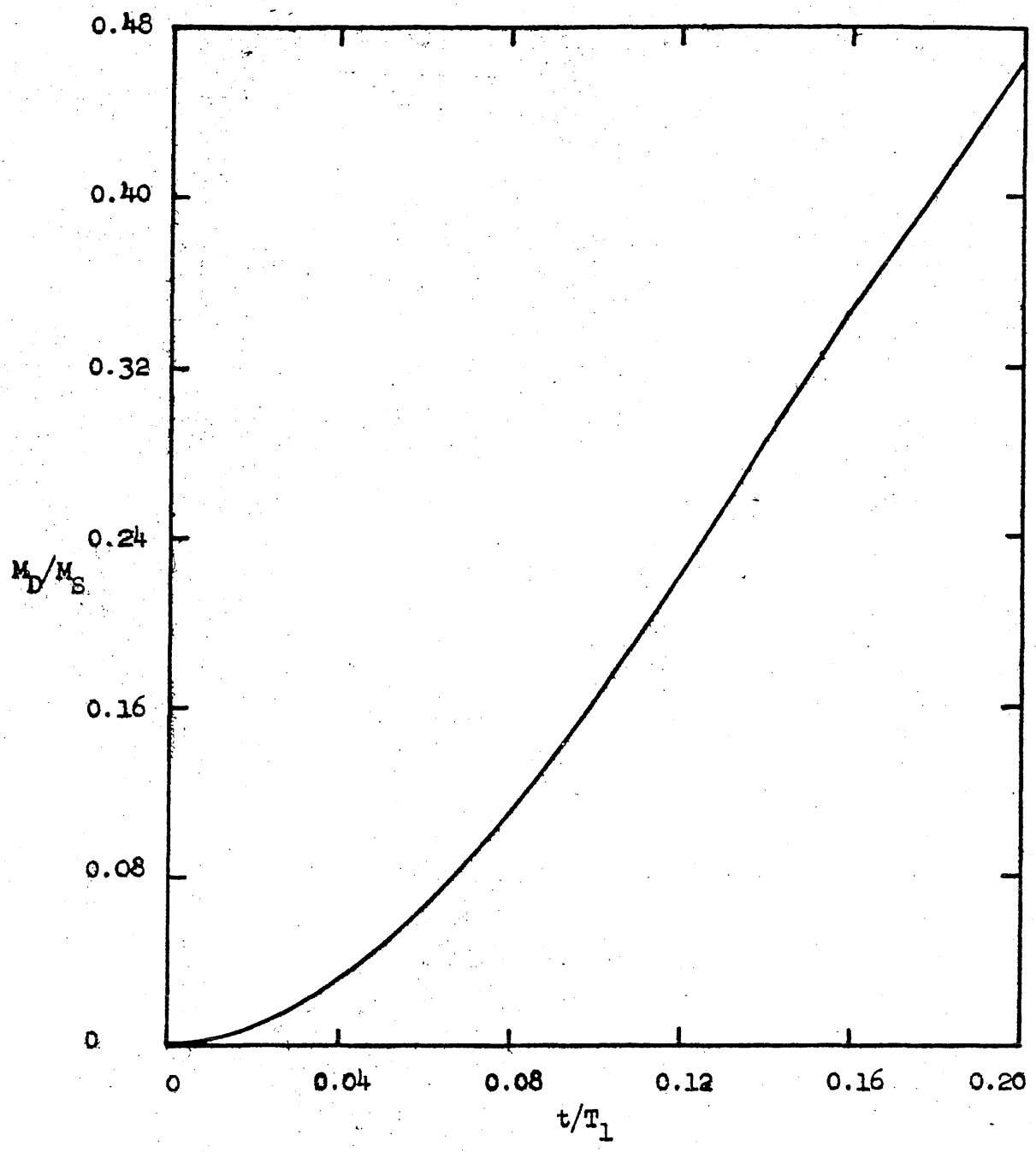

Figure 12 - Ratio of Dynamic Center Moment to Maximum Static Center Moment Versus Time Parameter ($t_1/T_1 = 0.2$)

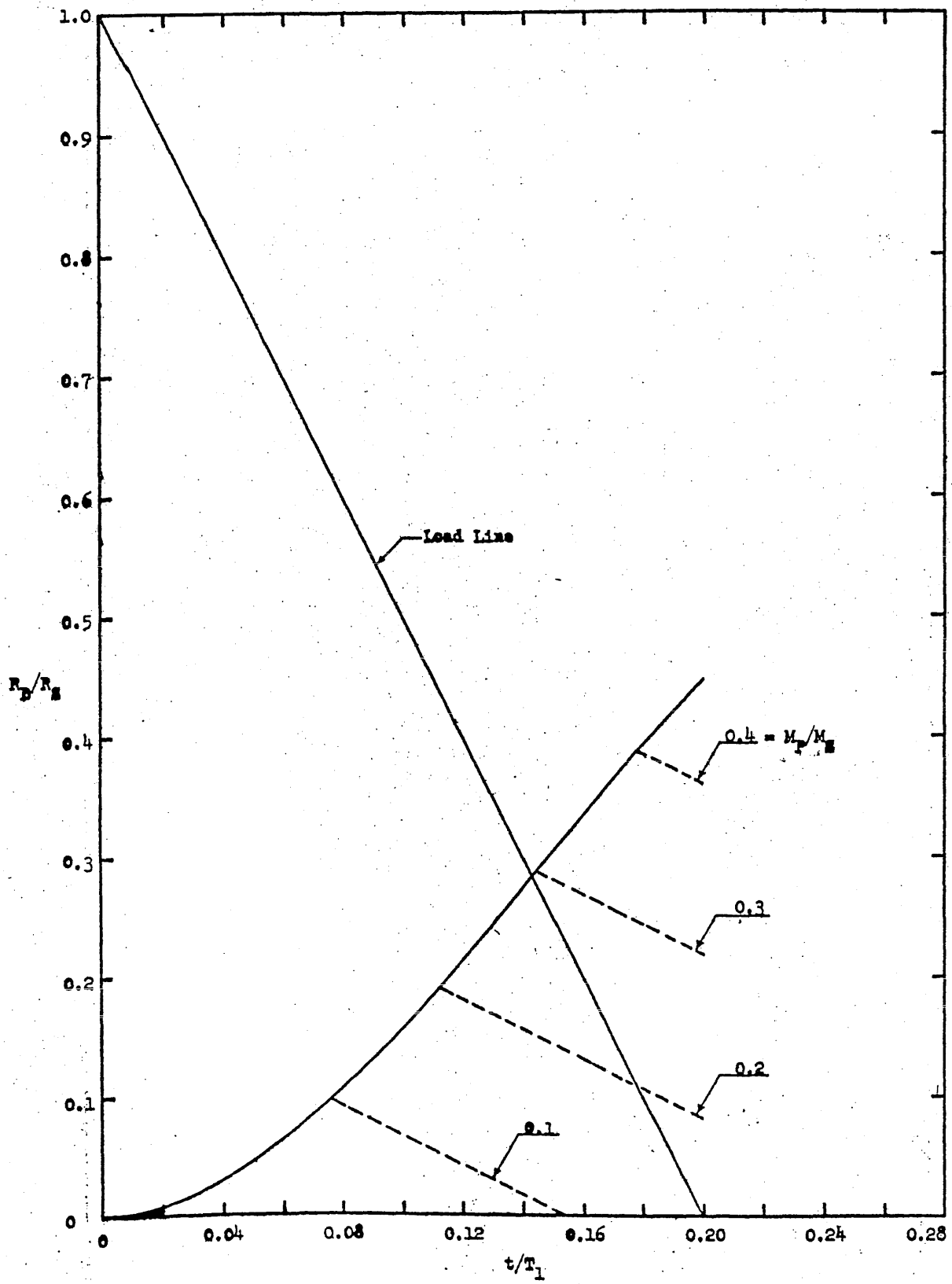

Figure 13 - Ratio of Dynamic End Reaction to Maximum Static End Reaction Versus Time Parameter ($t_1/T_1 = 0.2$)

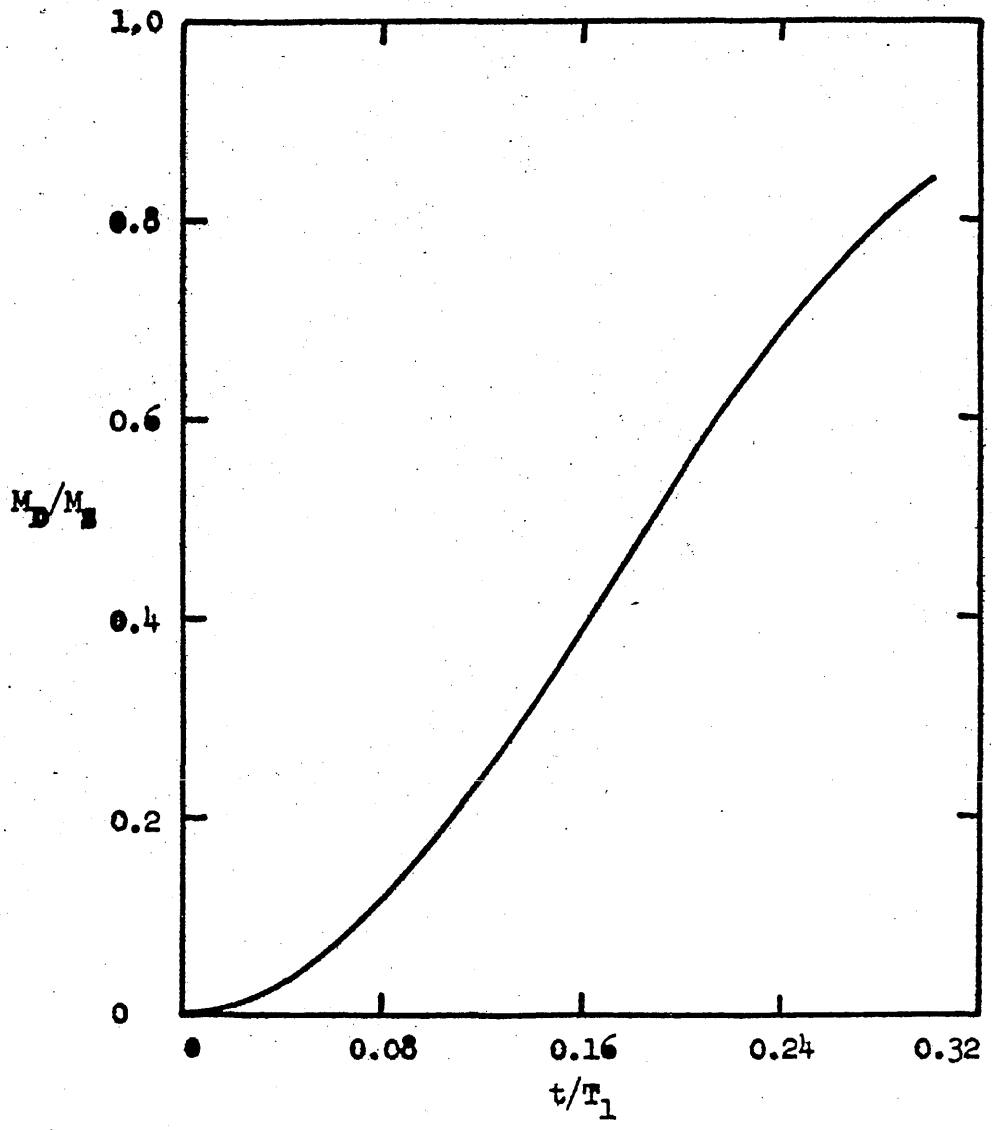

Figure 14 - Ratio of Dynamic Center Moment to Maximum Static Center Moment Versus Time Parameter ($t_1/T_1 = 0.3$)

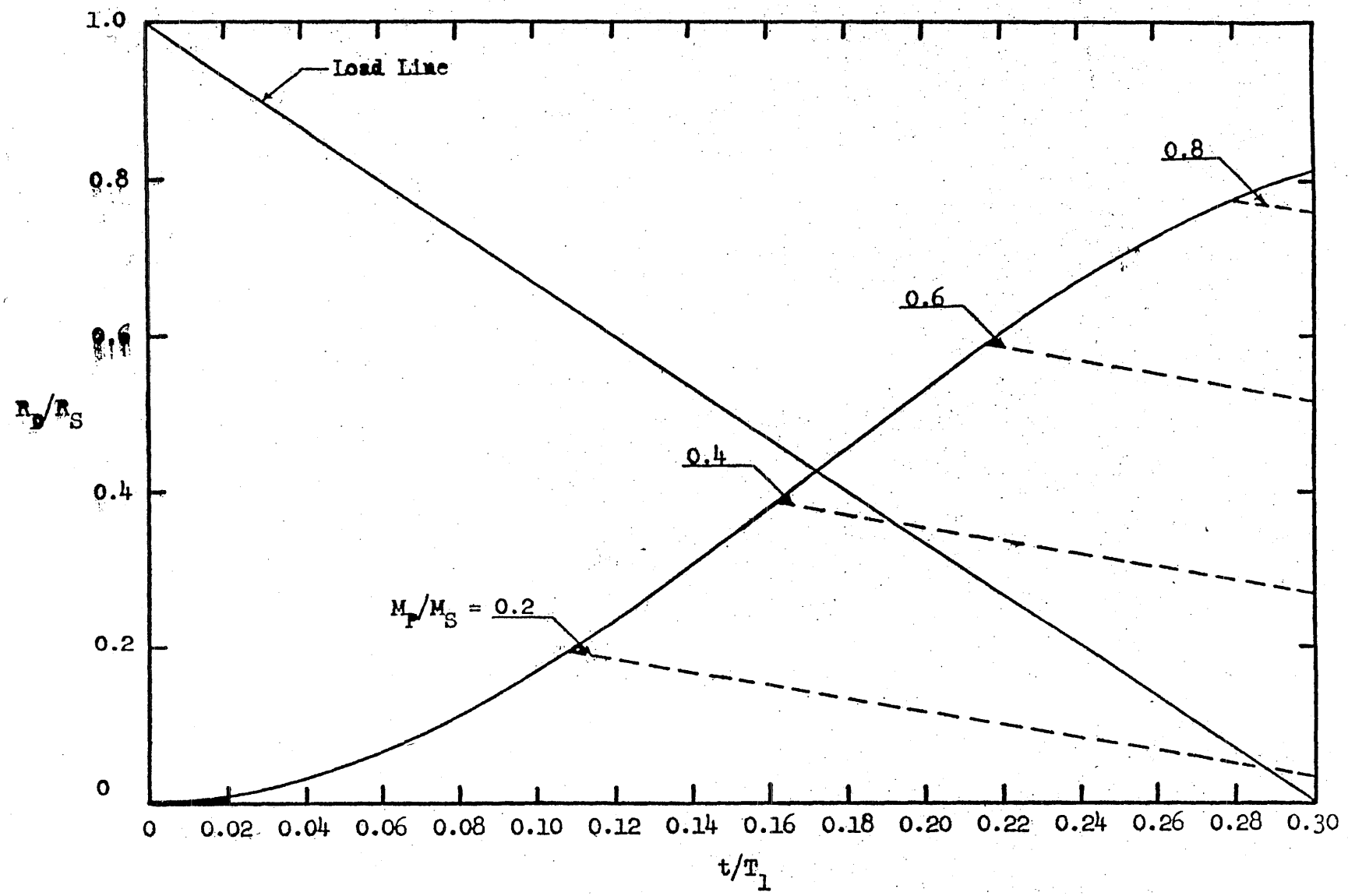

Figure 15 - Ratio of Dynamic End Reaction to Maximum Static End Reaction Versus Time Parameter ($t_1/T_1 = 0.3$)

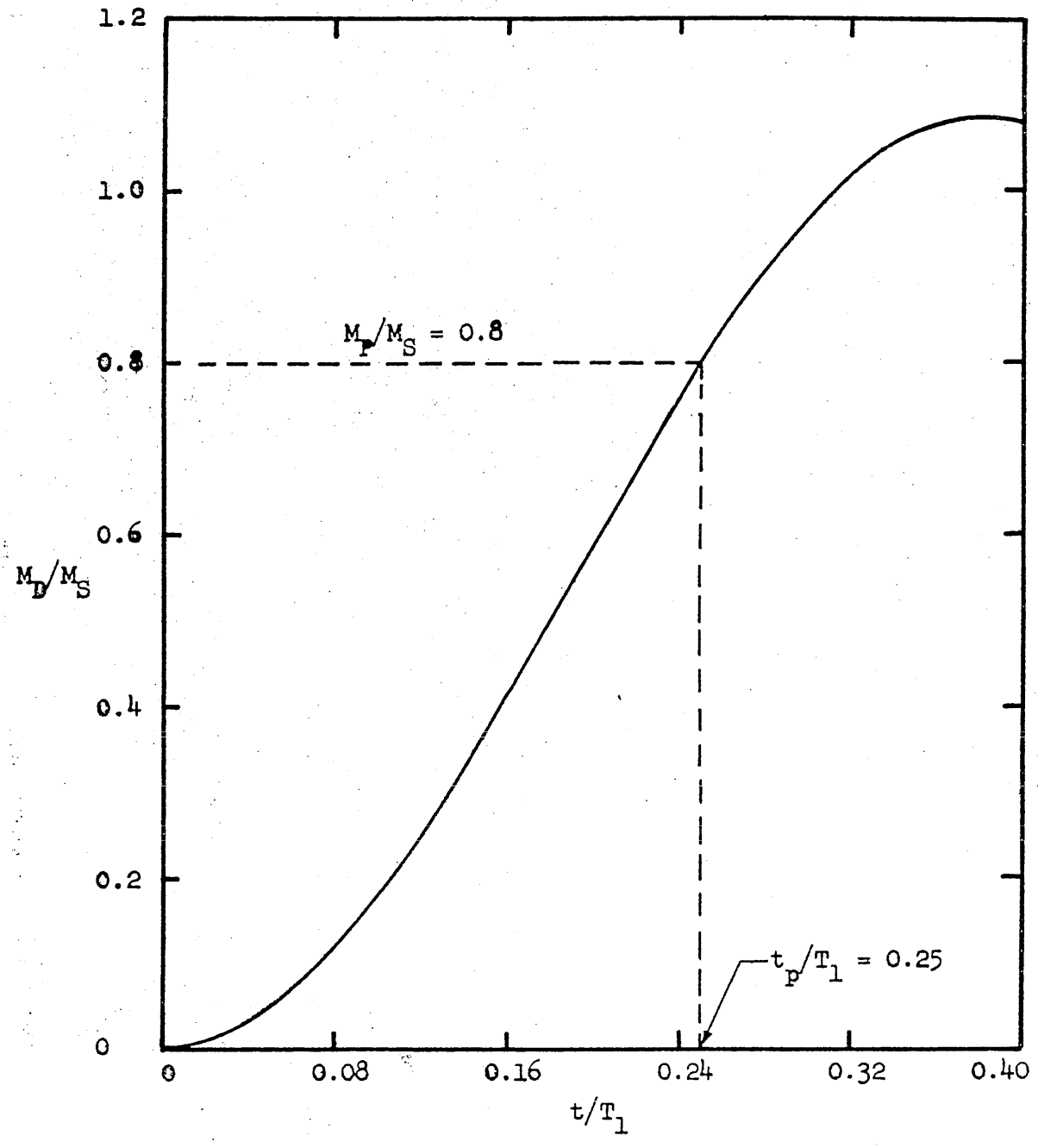

Figure 16 - Ratio of Dynamic Center Moment to Maximum Static Center Moment Versus Time Parameter ($t_1/T_1 = 0.4$)

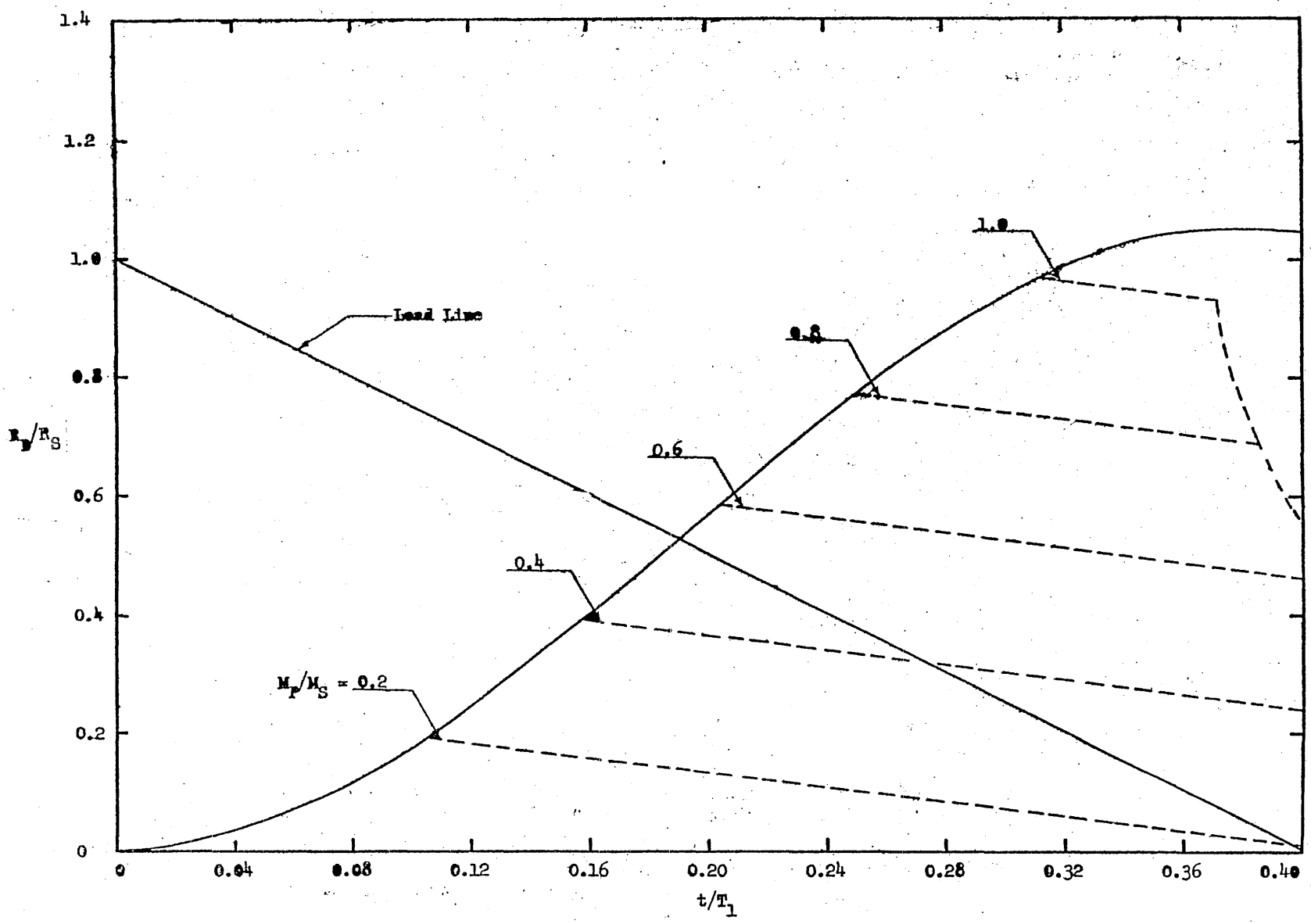

Figure 17 - Ratio of Dynamic End Reaction to Maximum Static End Reaction Versus Time Parameter (t_1/T_1 = 0.4)

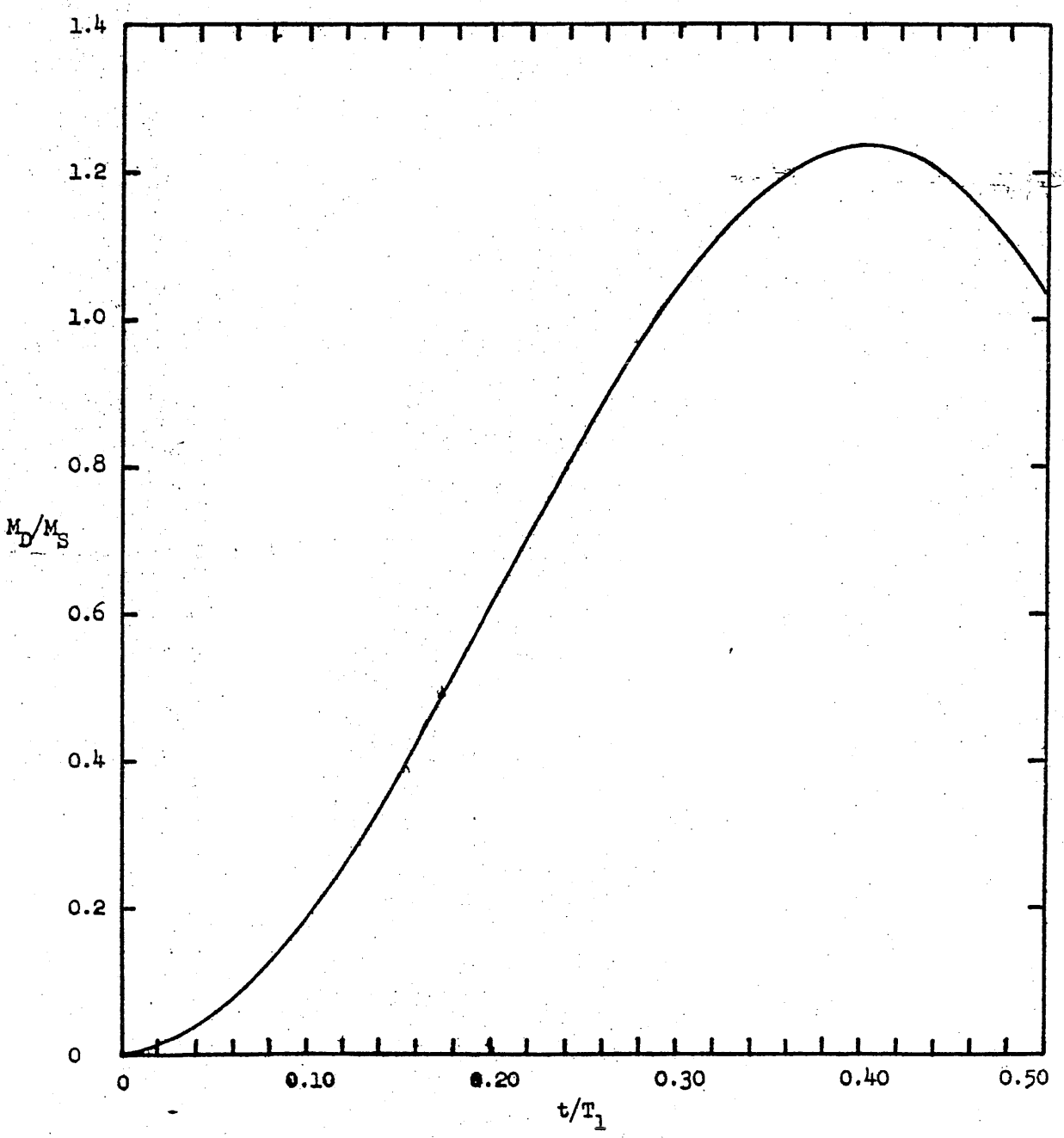

Figure 18 - Ratio of Dynamic Center Moment to Maximum Static Center Moment Versus Time Parameter ($t_1/T_1 = 0.5$)

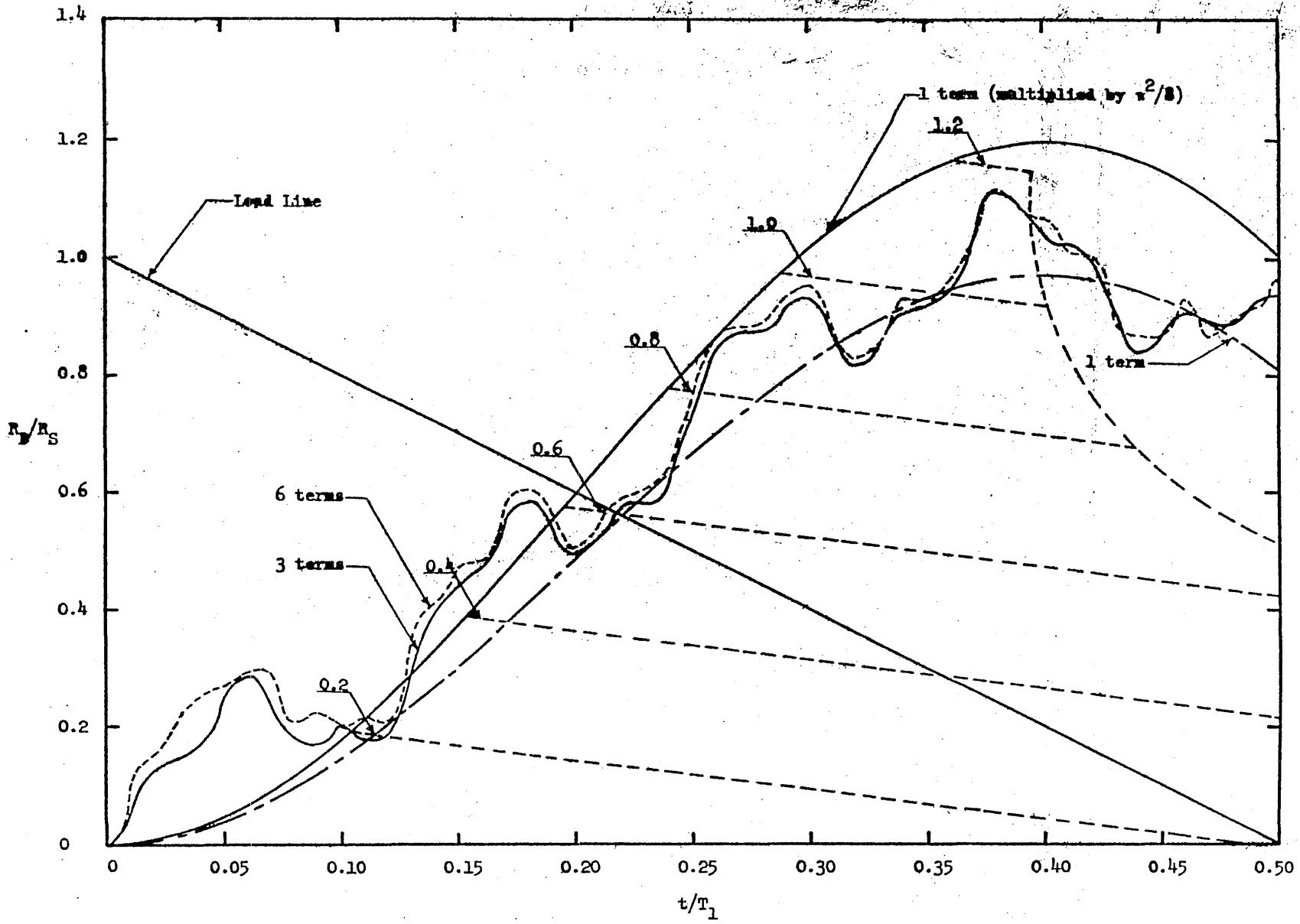

Figure 19 - Ratio of Dynamic End Reaction to Maximum Static End Reaction Versus Time Parameter ($t_1/T_1 = 0.5$)

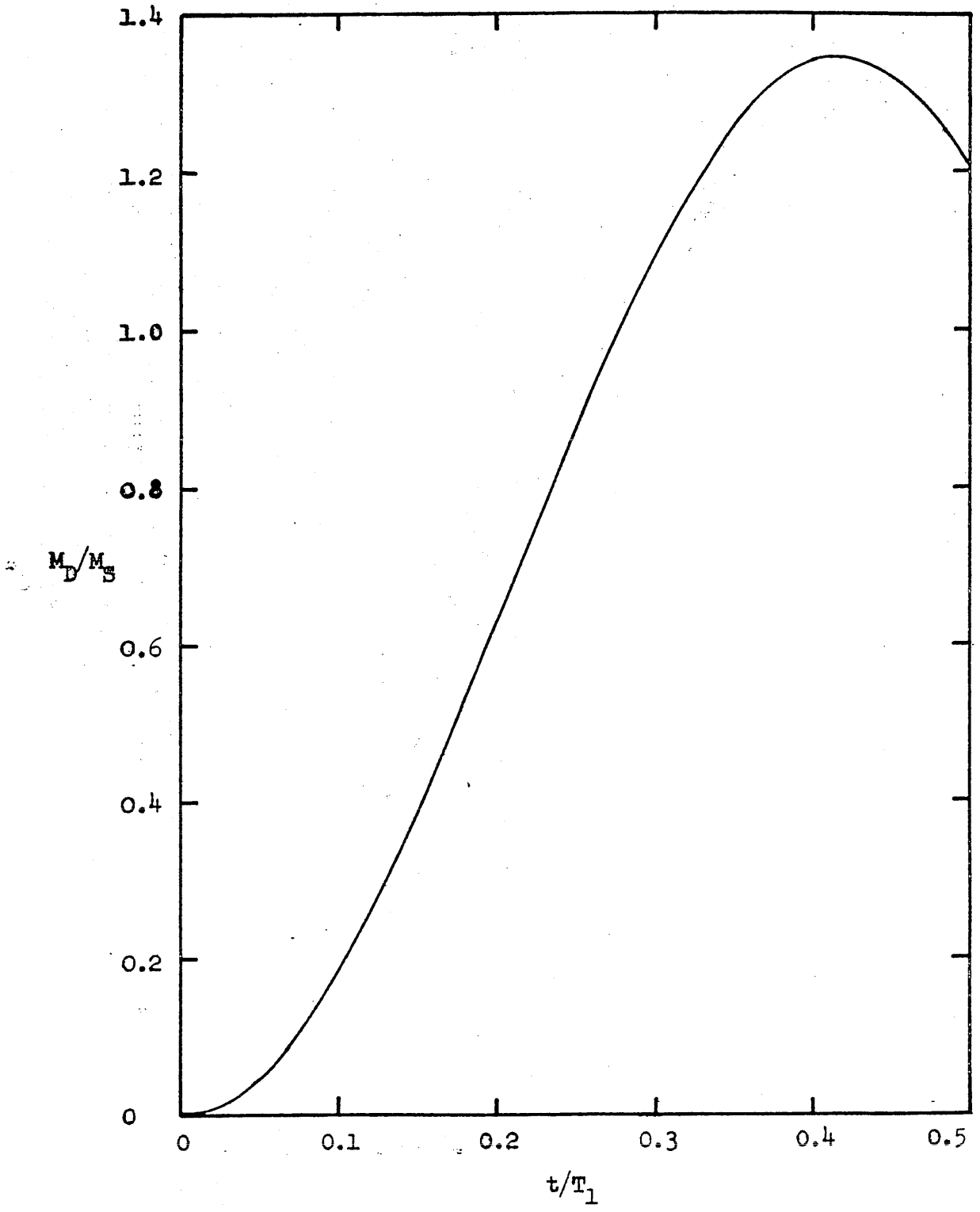

Figure 20 - Ratio of Dynamic Center Moment to Maximum Static Center Moment Versus Time Parameter ($t_1/T_1 = 0.6$)

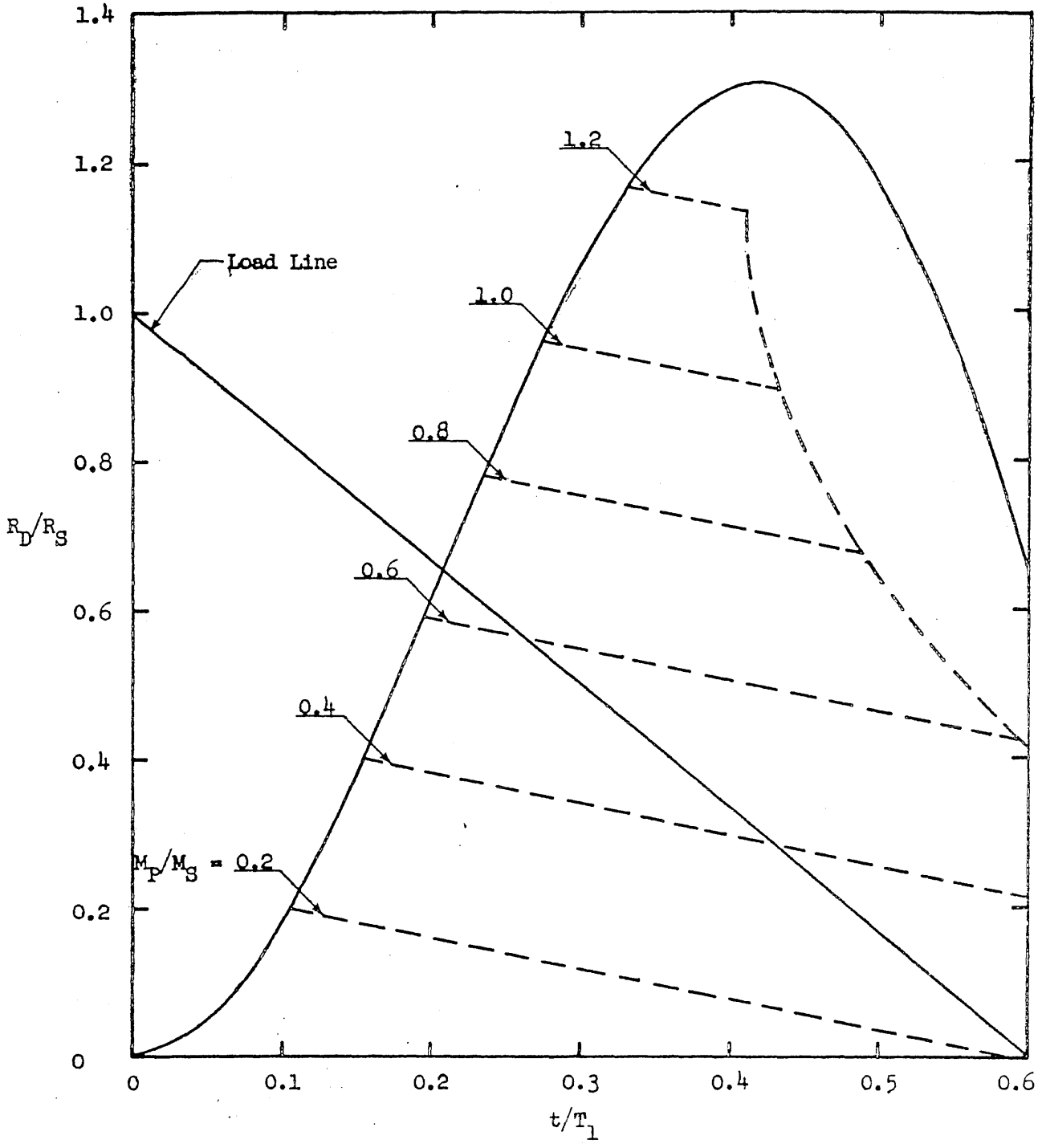

Figure 21 - Ratio of Dynamic End Reaction to Maximum Static End Reaction Versus Time Parameter (t_1/T_1 = 0.6)

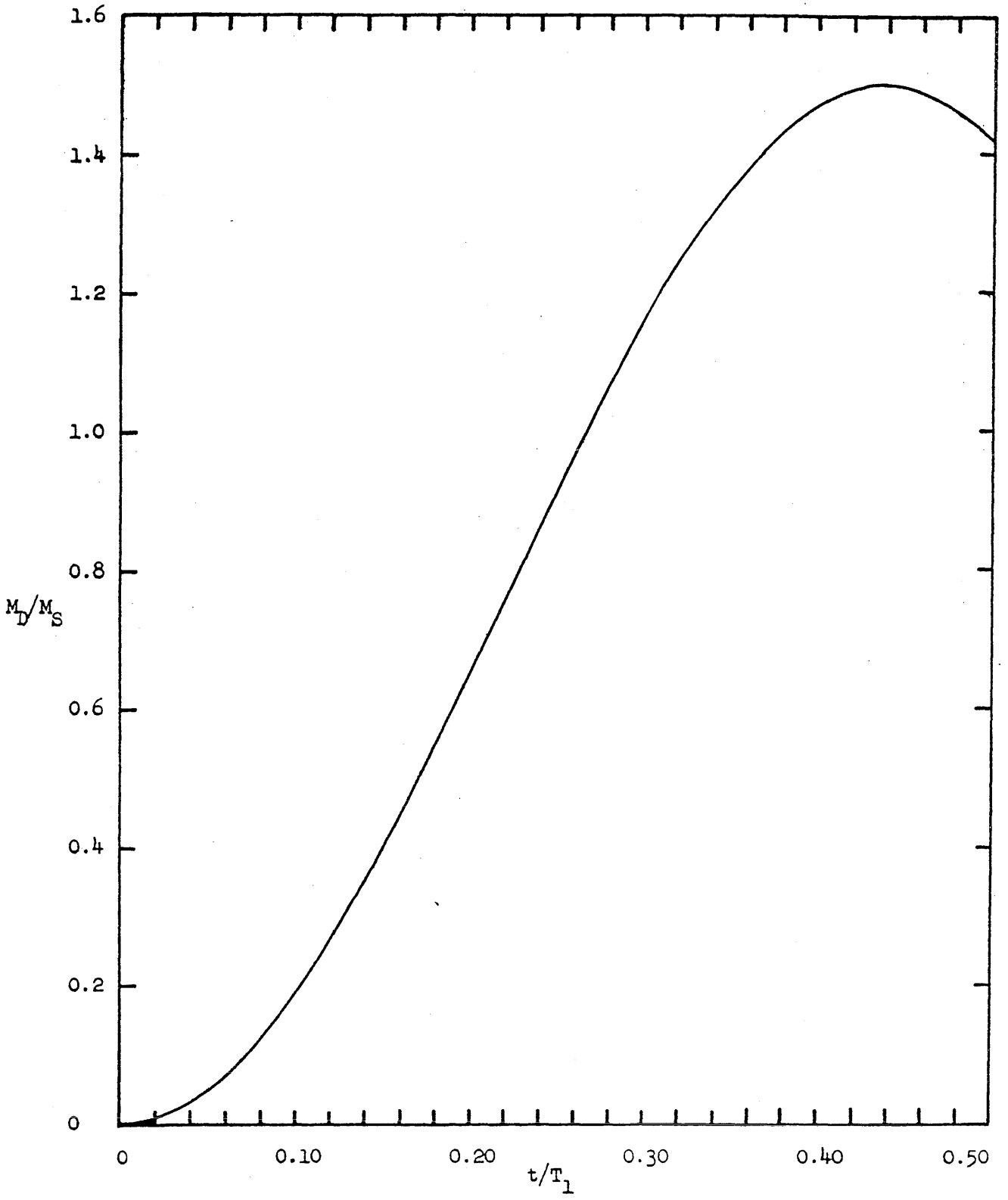

Figure 22 - Ratio of Dynamic Center Moment to Maximum Static Center Moment Versus Time Parameter ($t_1/T_1 = 0.8$)

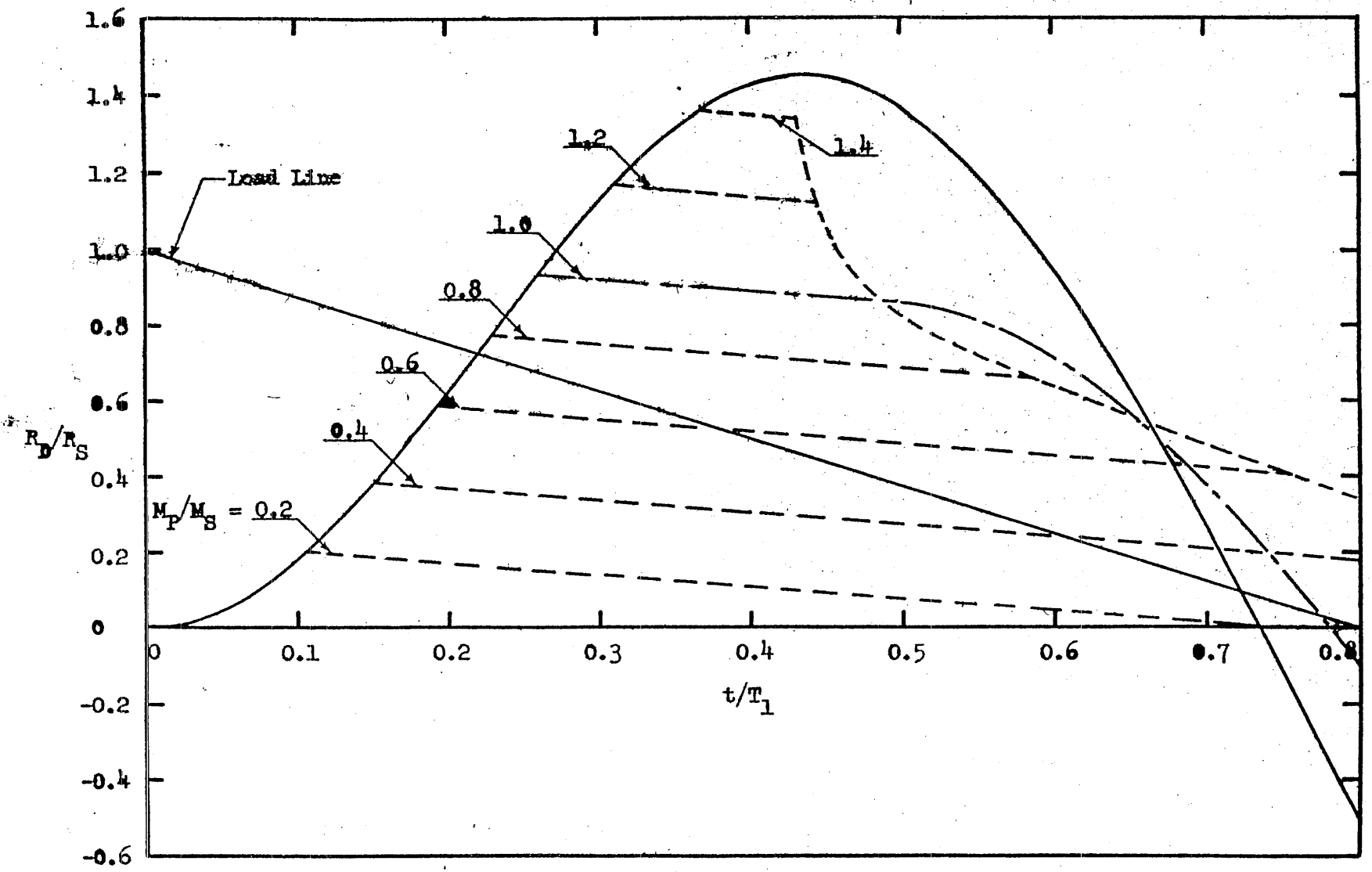

Figure 23 - Ratio of Dynamic End Reaction to Maximum Static End Reaction Versus Time Parameter (t_1/T_1 = 0.8)

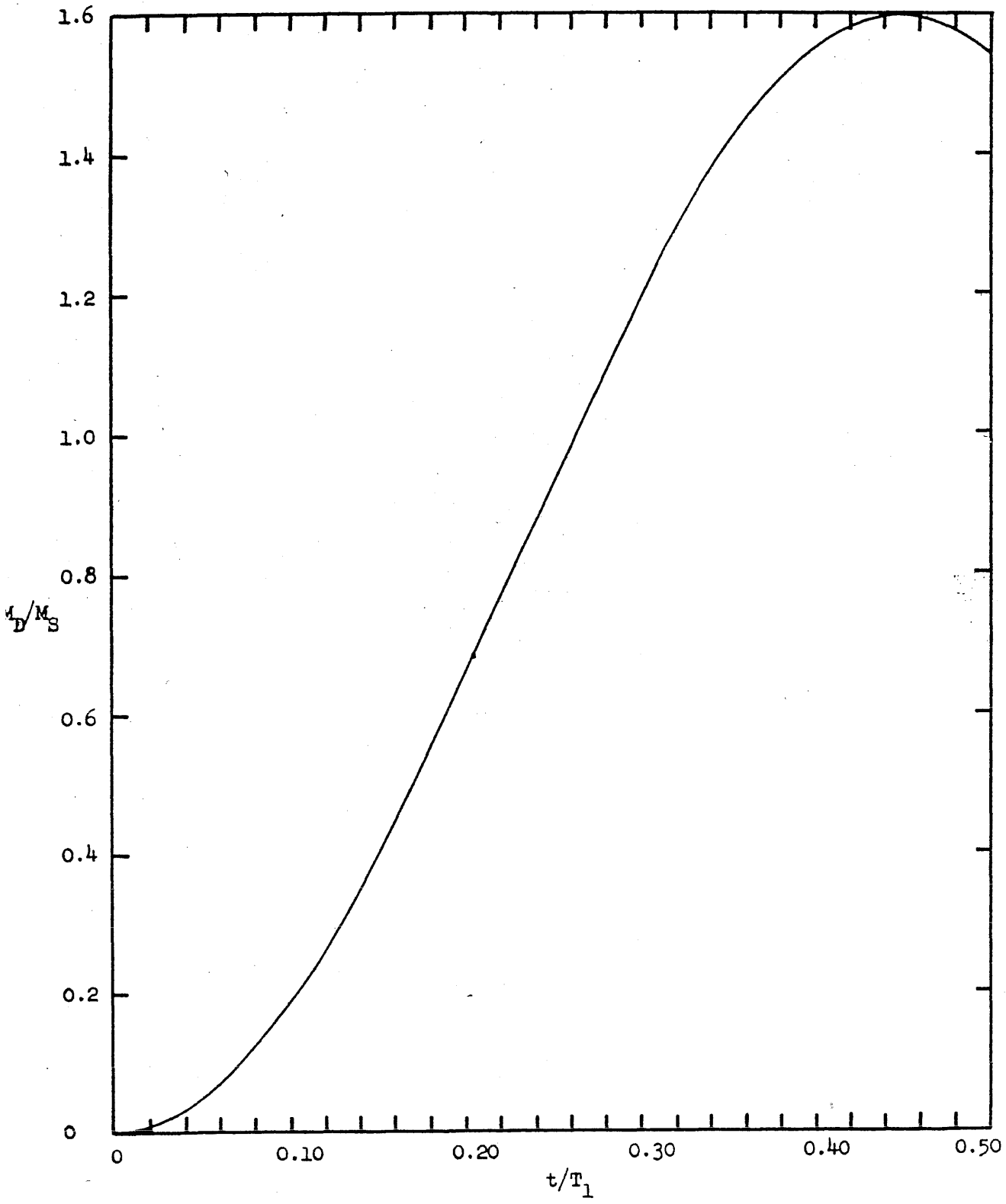

Figure 24 - Ratio of Dynamic Center Moment to Maximum Static Center Moment Versus Time Parameter ($t_1/T_1 = 1.0$)

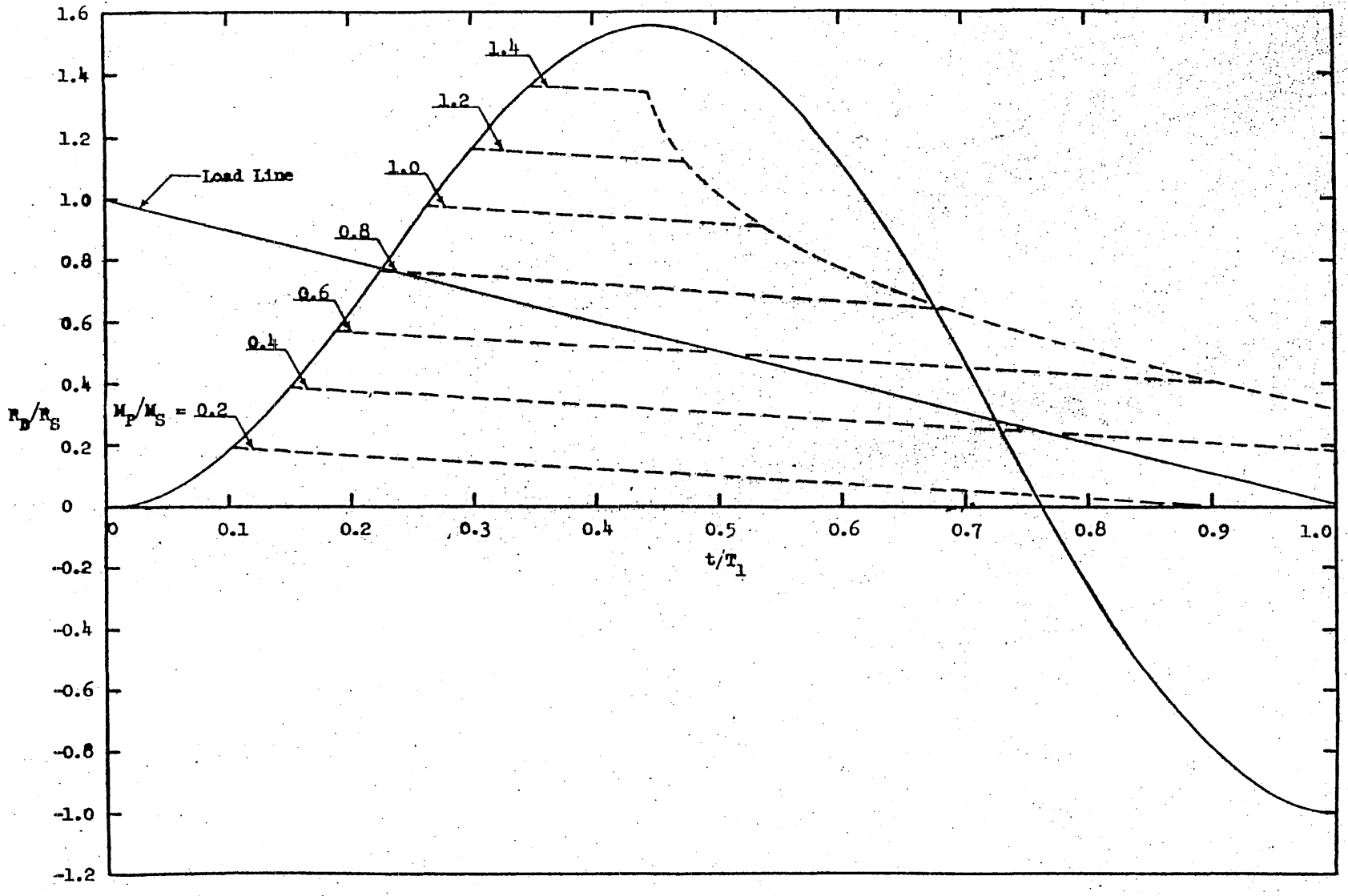

Figure 25 - Ratio of Dynamic End Reaction to Maximum Static End Reaction Versus Time Parameter (t_1/T_1 = 1.0)

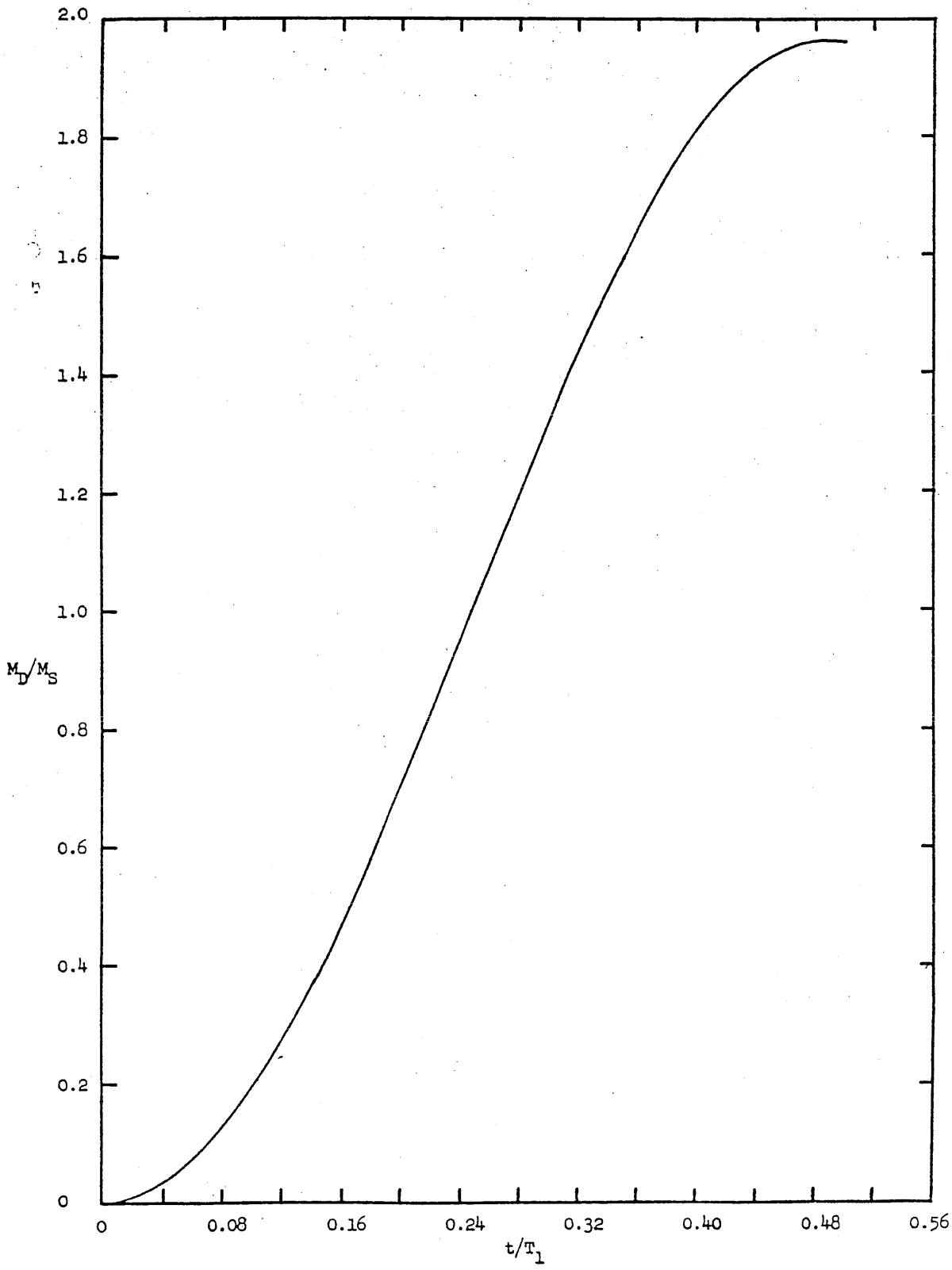

Figure 26 - Ratio of Dynamic Center Moment to Maximum Static Center Moment Versus Time Parameter ($t_1/T_1 = 5.0$)

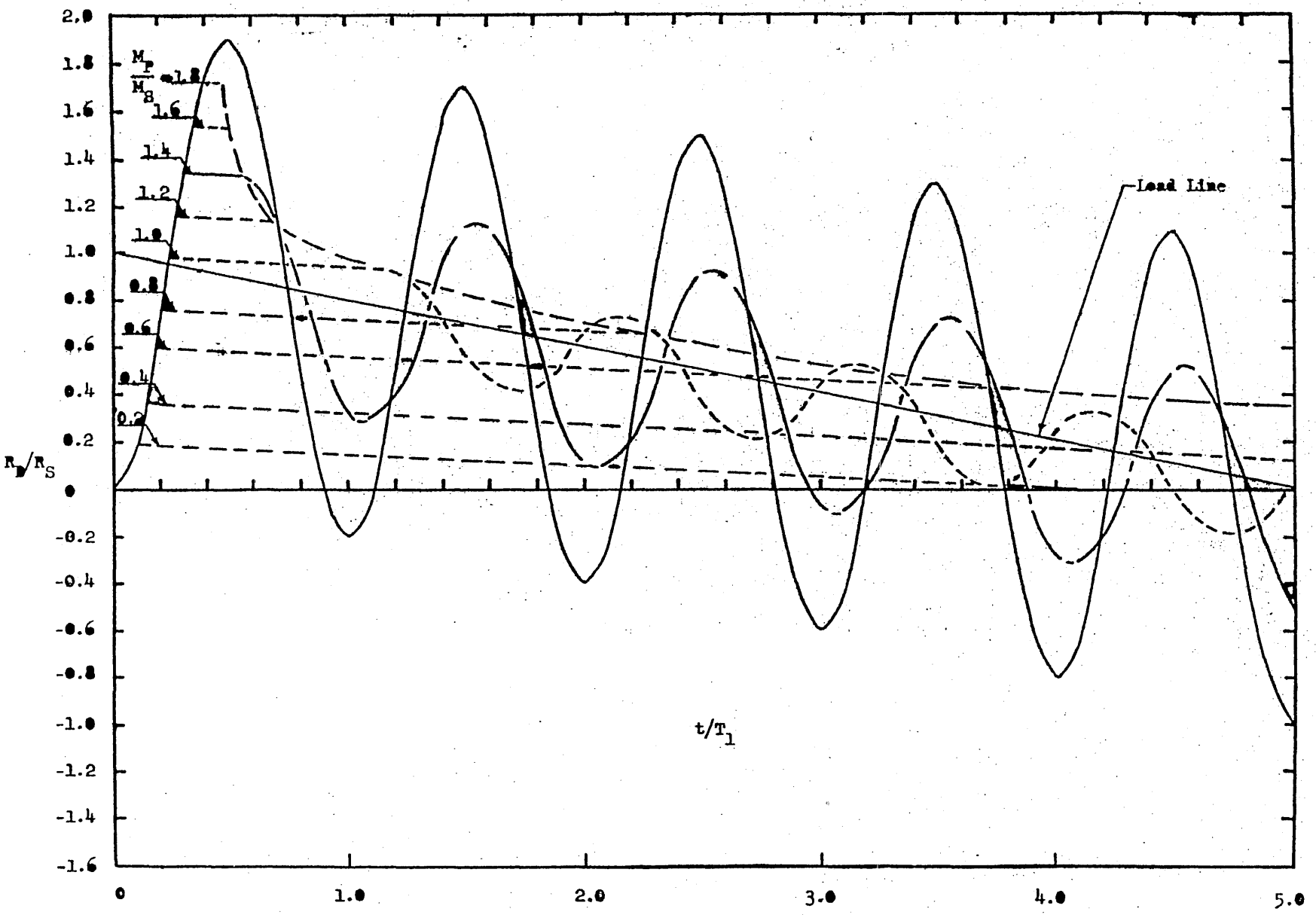

Figure 27 - Ratio of Dynamic End Reaction to Maximum Static End Reaction Versus Time Parameter ($t_1/T_1 = 5.0$)

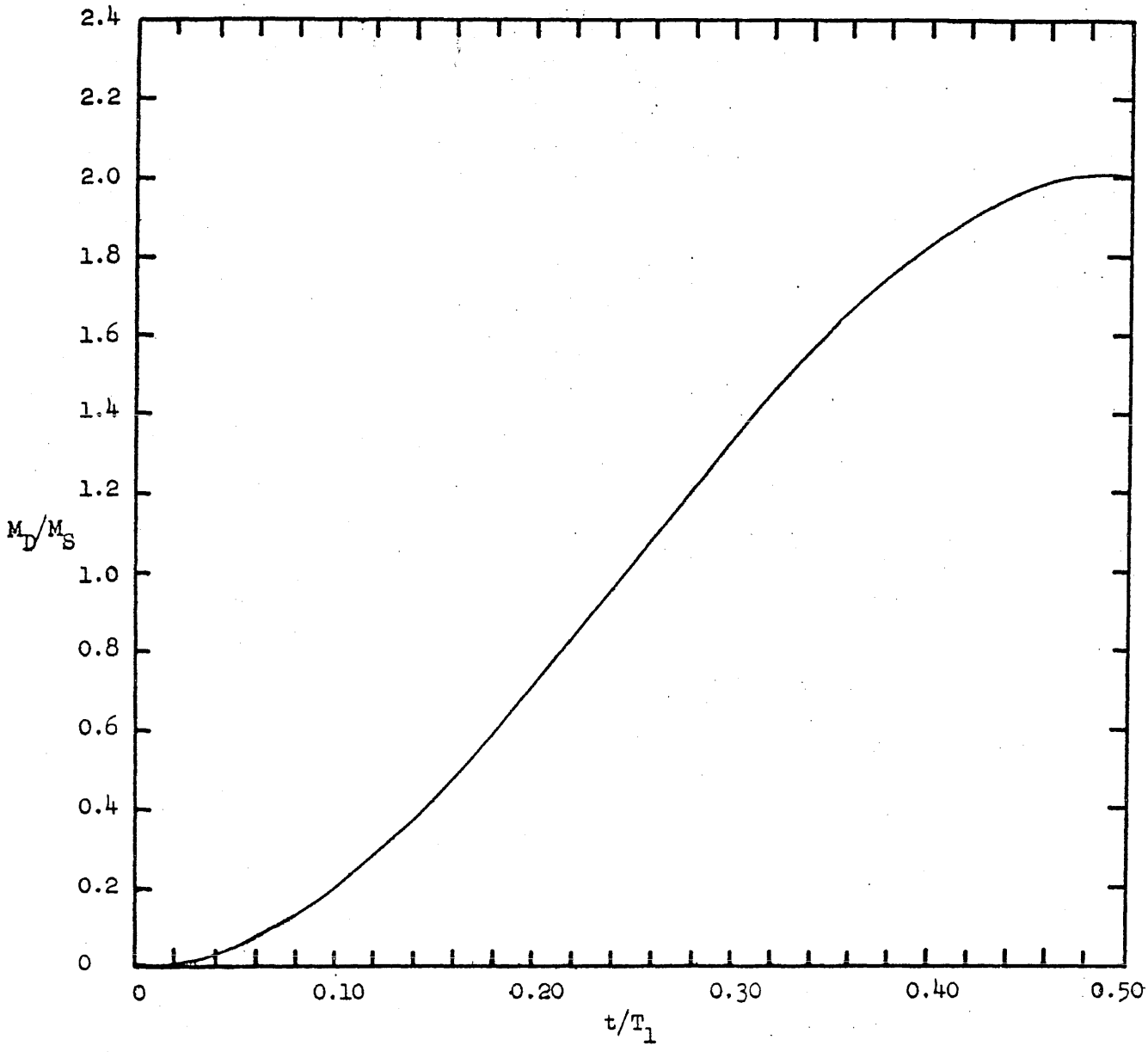

Figure 28 - Ratio of Dynamic Center Moment to Maximum Static Center Moment Versus Time Parameter (t_1/T_1 = 10.0)

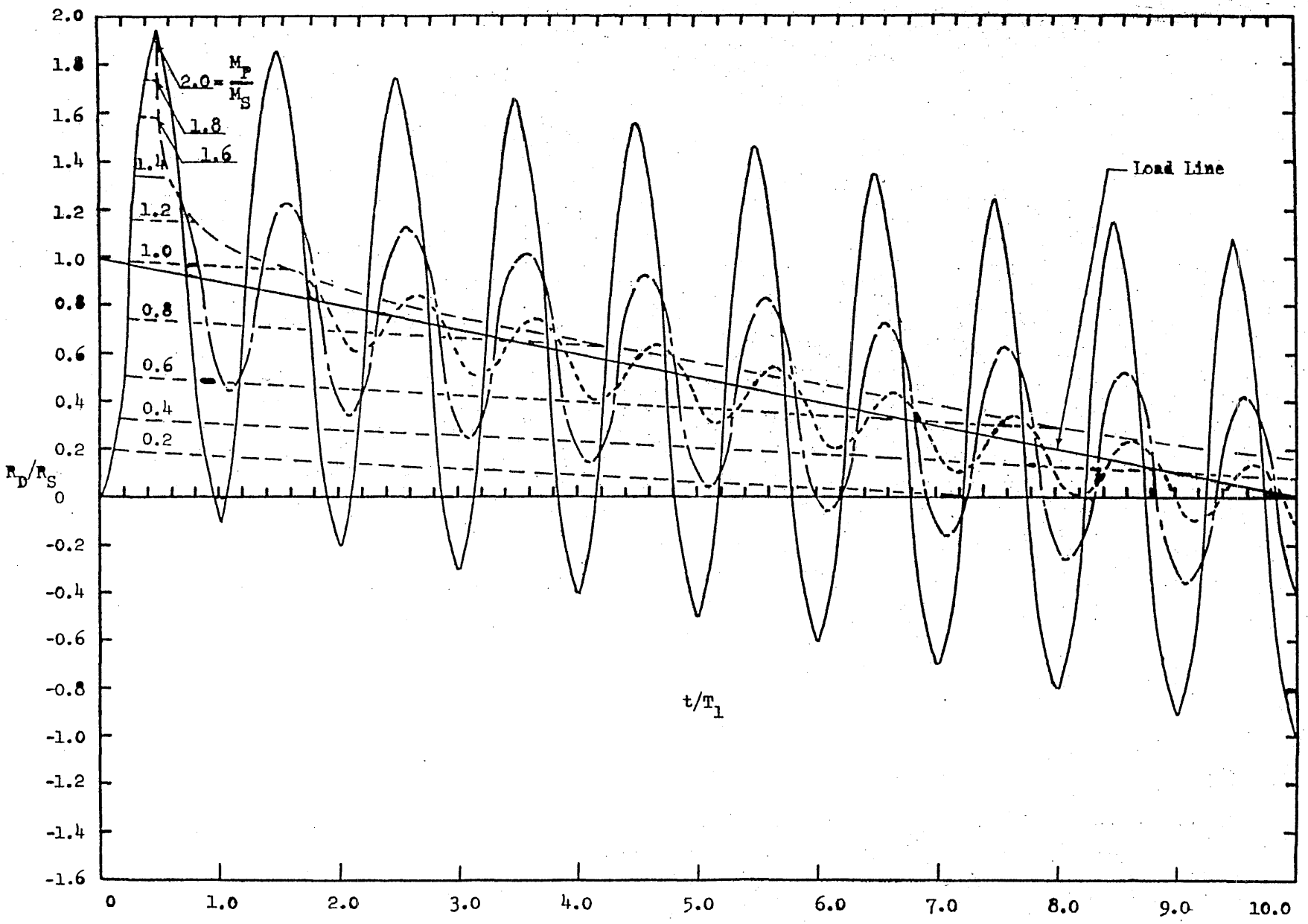

Figure 29 - Ratio of Dynamic End Reaction to Maximum Static End Reaction Versus Time Parameter ($t_1/T_1 = 10.0$)

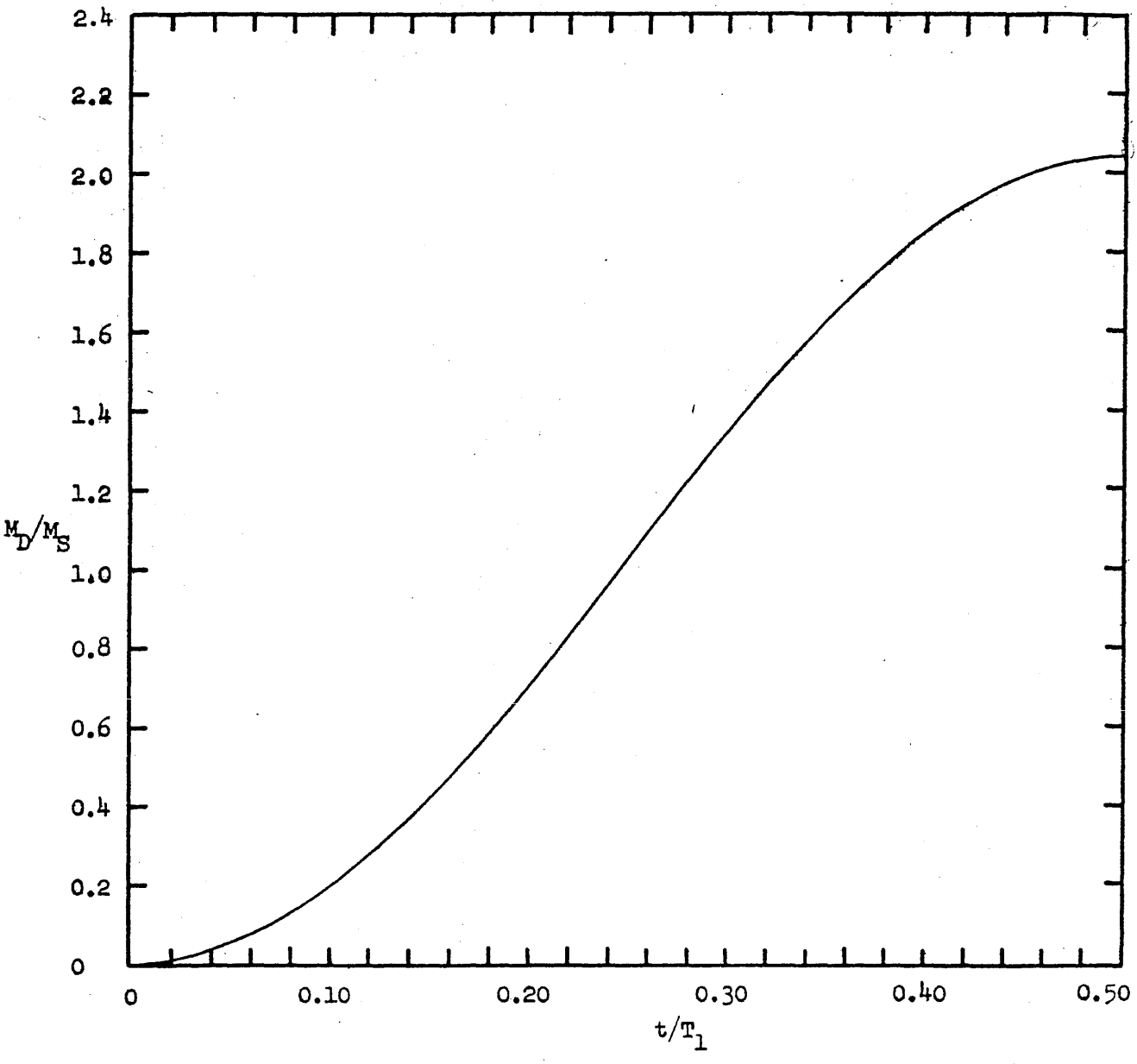

Figure 30 - Ratio of Dynamic Center Moment to Maximum Static Center Moment Versus Time Parameter (t_1/T_1 = 20.0)

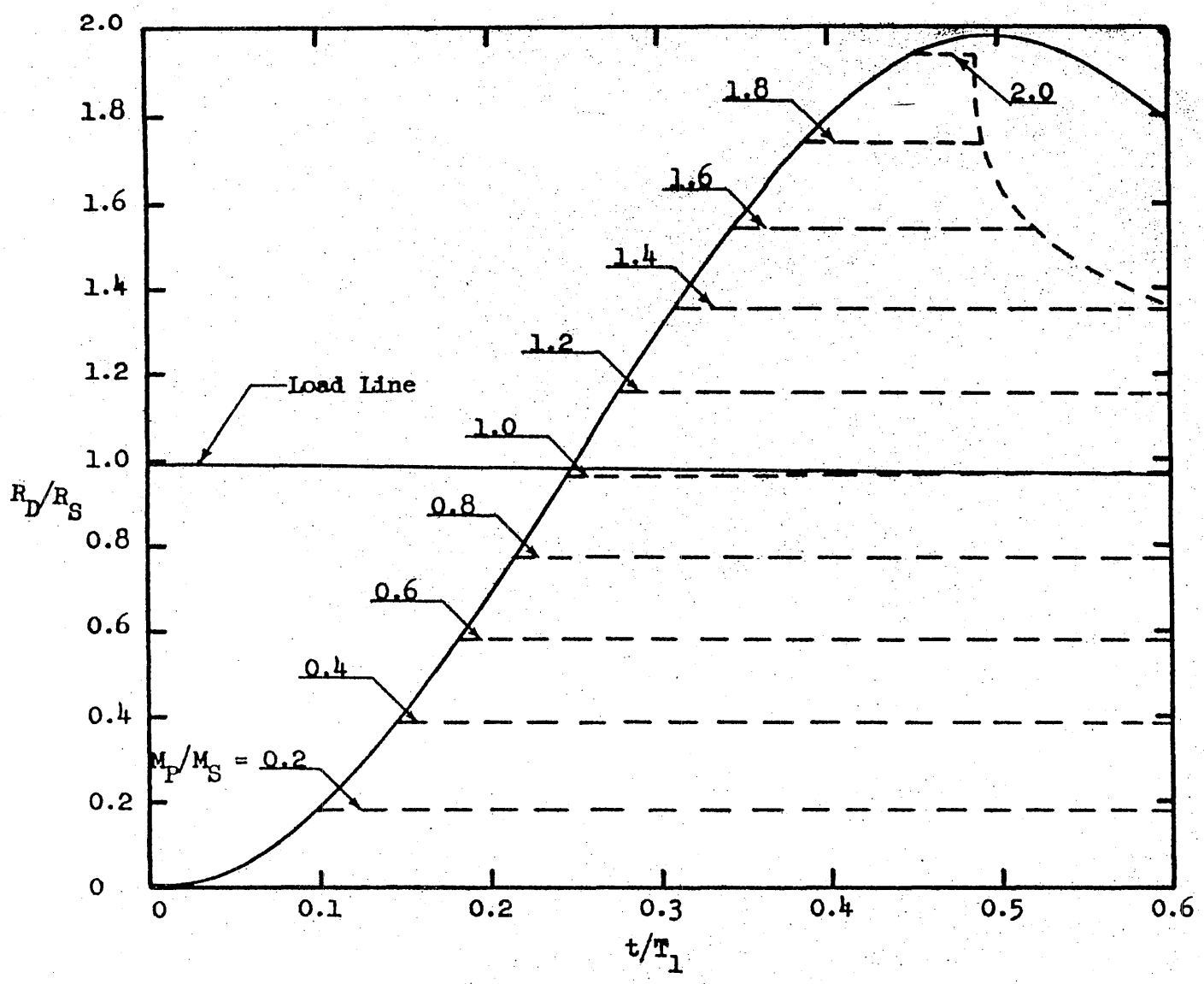

Figure 31 - Ratio of Dynamic End Reaction to Maximum Static End Reaction Versus Time Parameter (t_1/T_1 = 20.0)

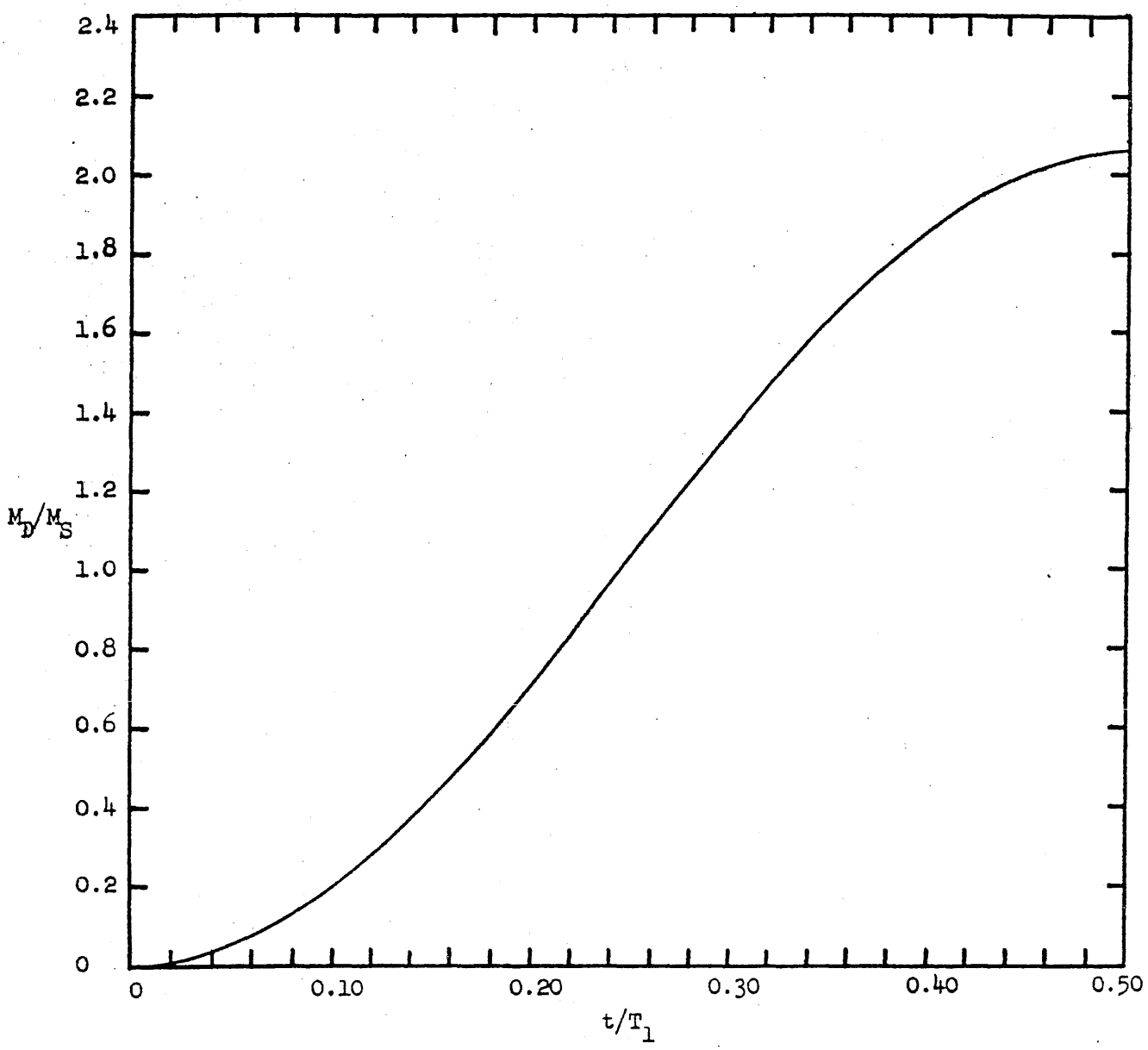

Figure 32 - Ratio of Dynamic Center Moment to Maximum Static Center Moment Versus Time Parameter (t_1/T_1 = 50.0)

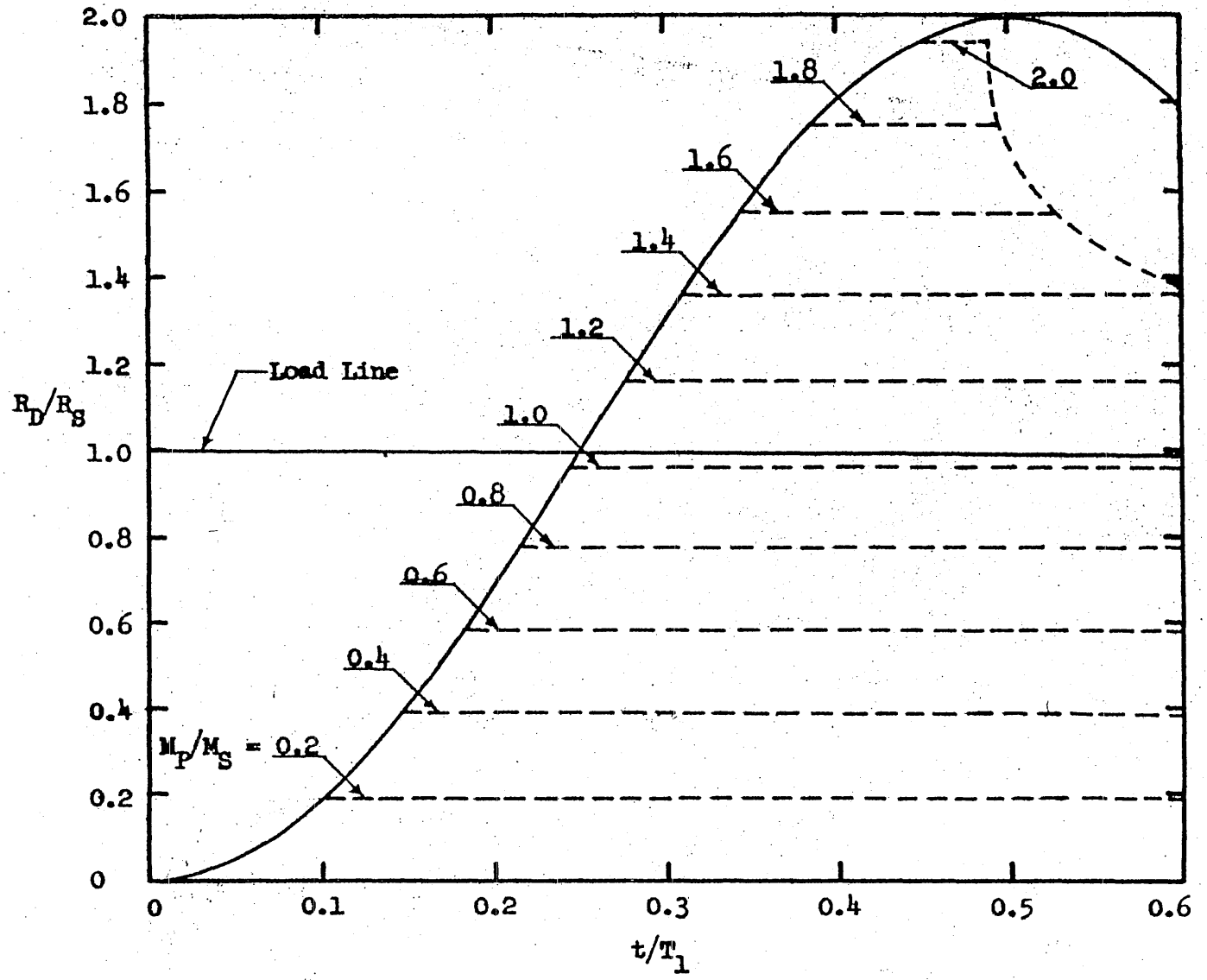

Figure 33 - Ratio of Dynamic End Reaction to Maximum Static End Reaction Versus Time Parameter (t_1/T_1 = 50.0)

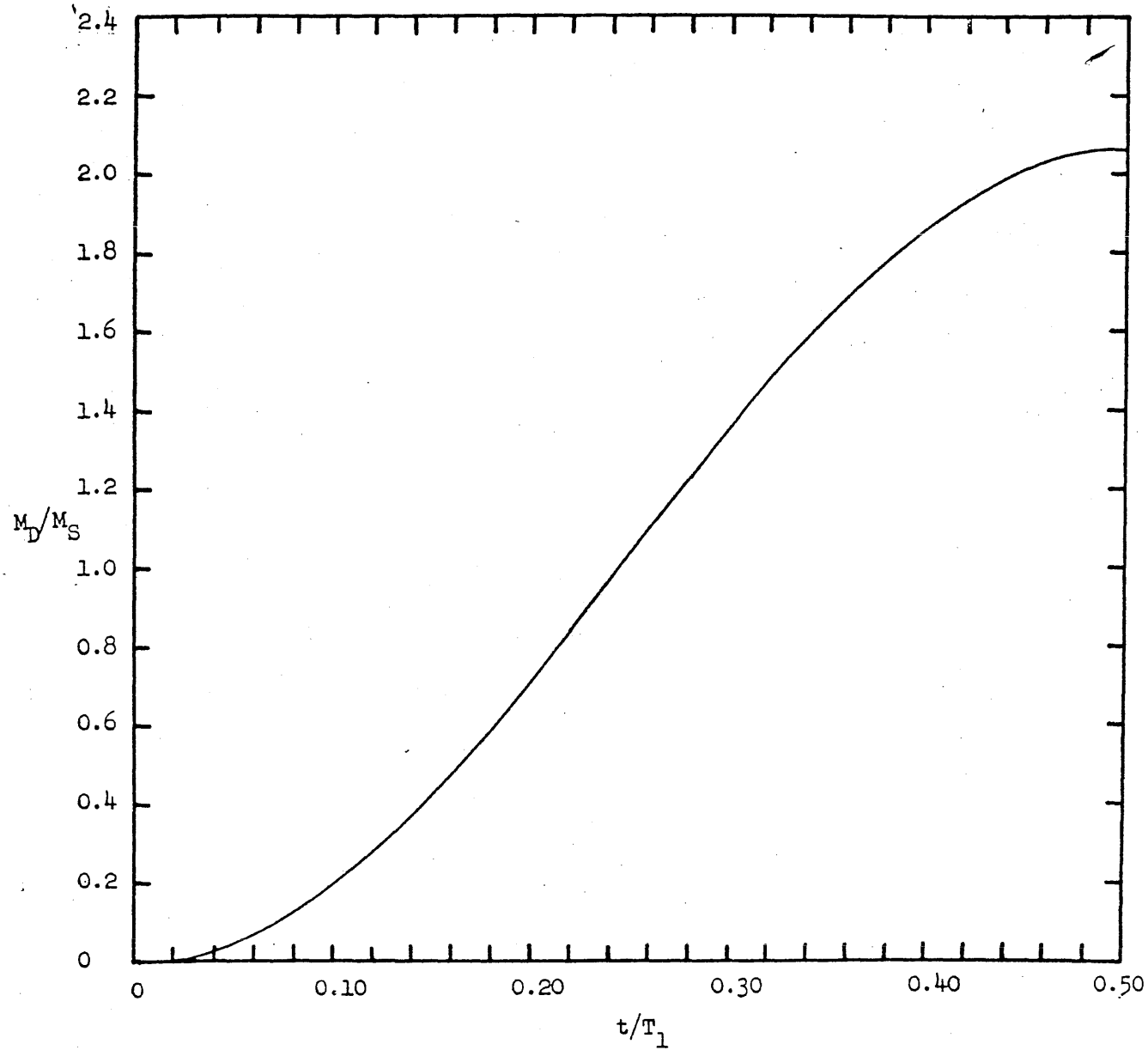

Figure 34 - Ratio of Dynamic Center Moment to Maximum Static Center Moment Versus Time Parameter (t_1/T_1 = 100.0)

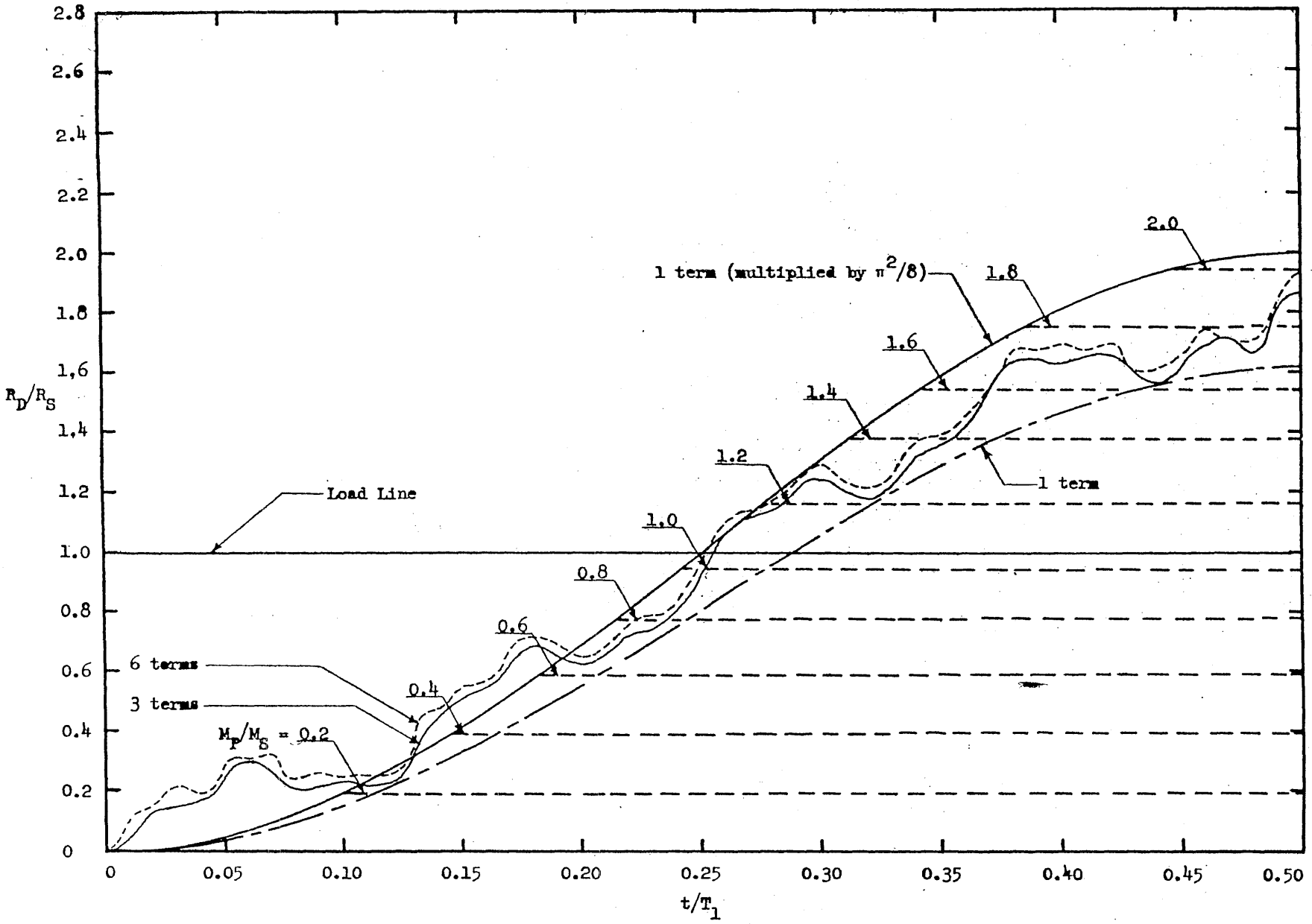

Figure 35 - Ratio of Dynamic End Reaction to Maximum Static End Reaction Versus Time Parameter (t_1/T_1 = 100.0)

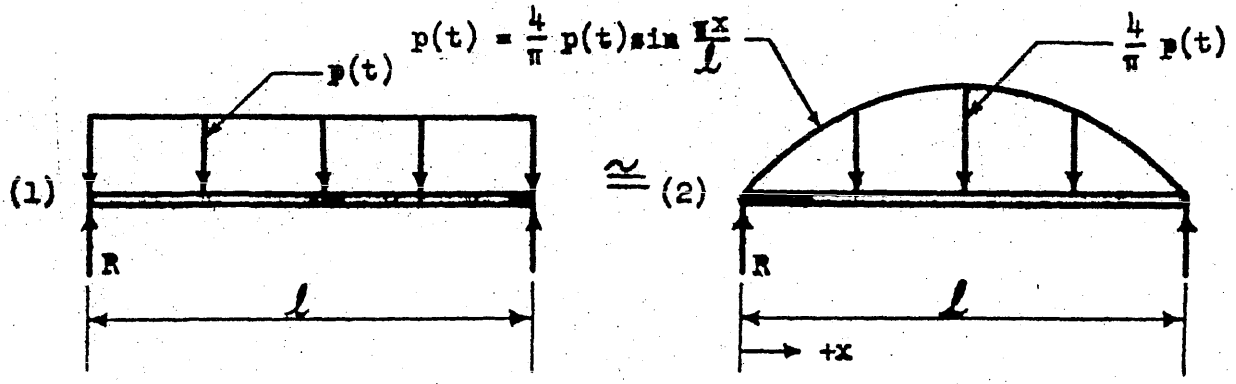

Figure 36 - Comparison of Actual and Equivalent Beam Loading

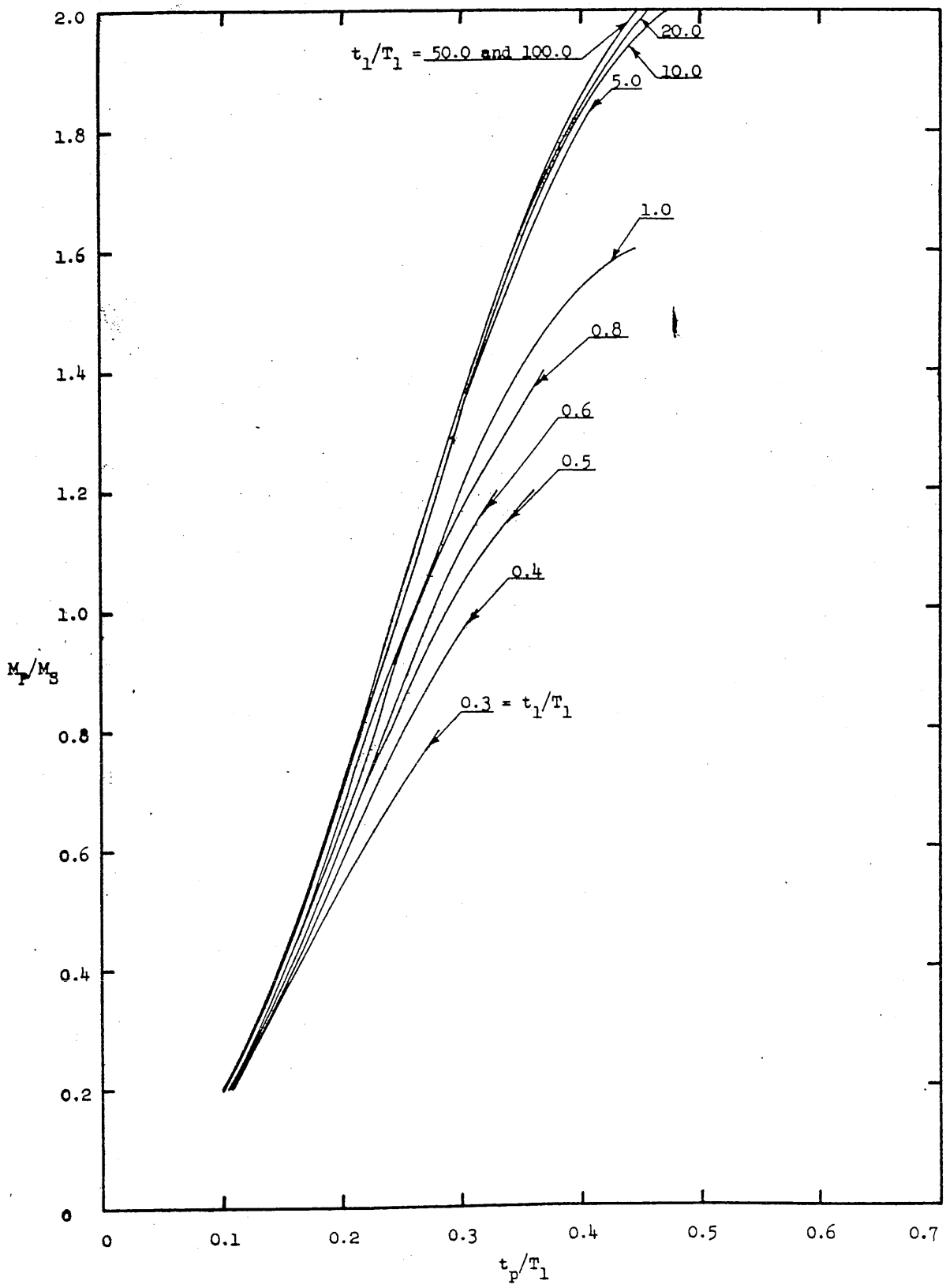

Figure 37 - Plot of Duration of Initial Elastic Phase (t_p/T_1) Versus Beam Resistance Parameter (M_P/M_S) for Fixed Values of Pulse Duration (t_1/T_1)

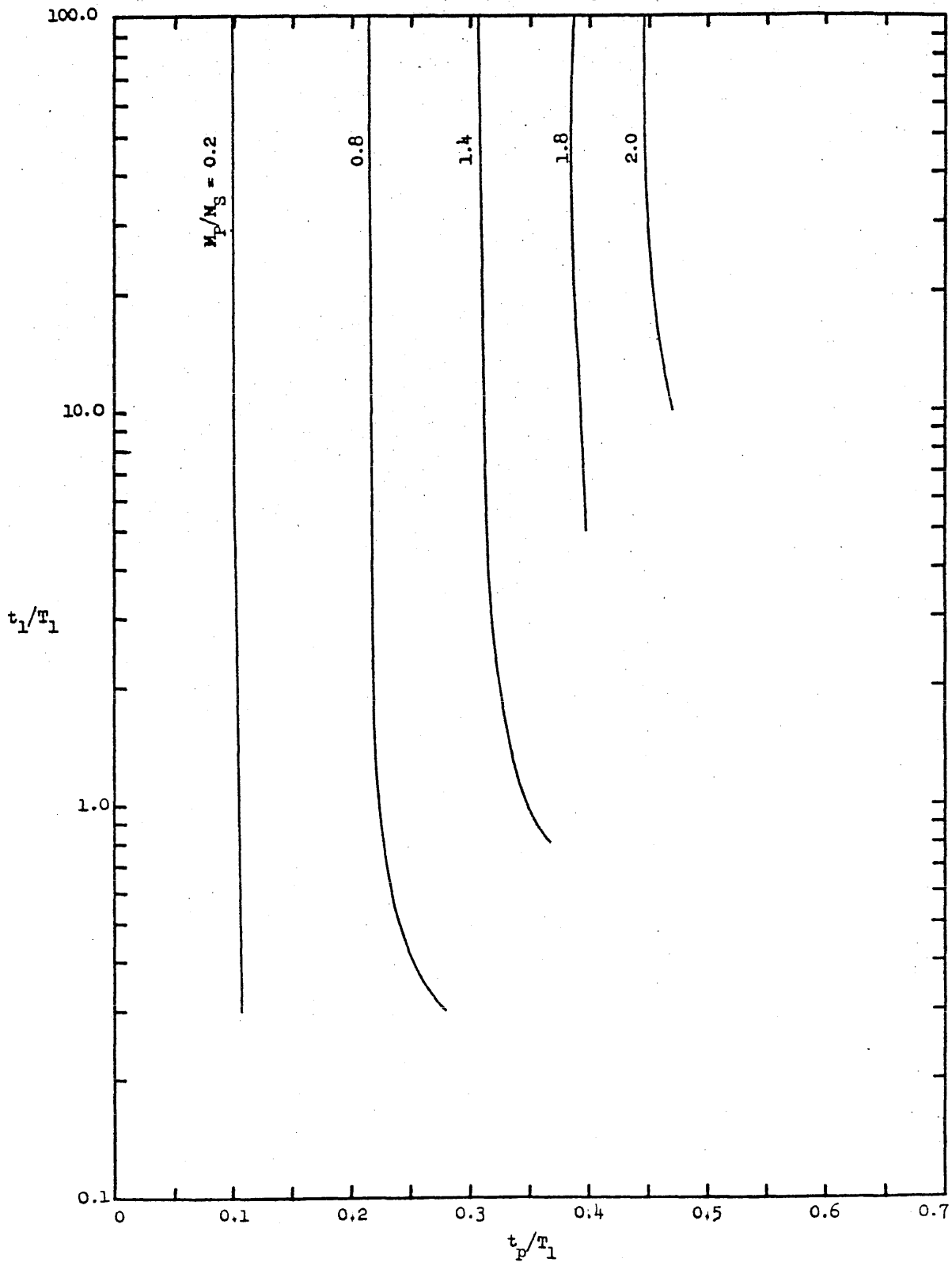

Figure 38 - Plot of Duration of Initial Elastic Phase (t_p/T_1) Versus Pulse Duration (t_1/T_1) for Fixed Values of Beam Resistance Parameter (M_p/M_s)

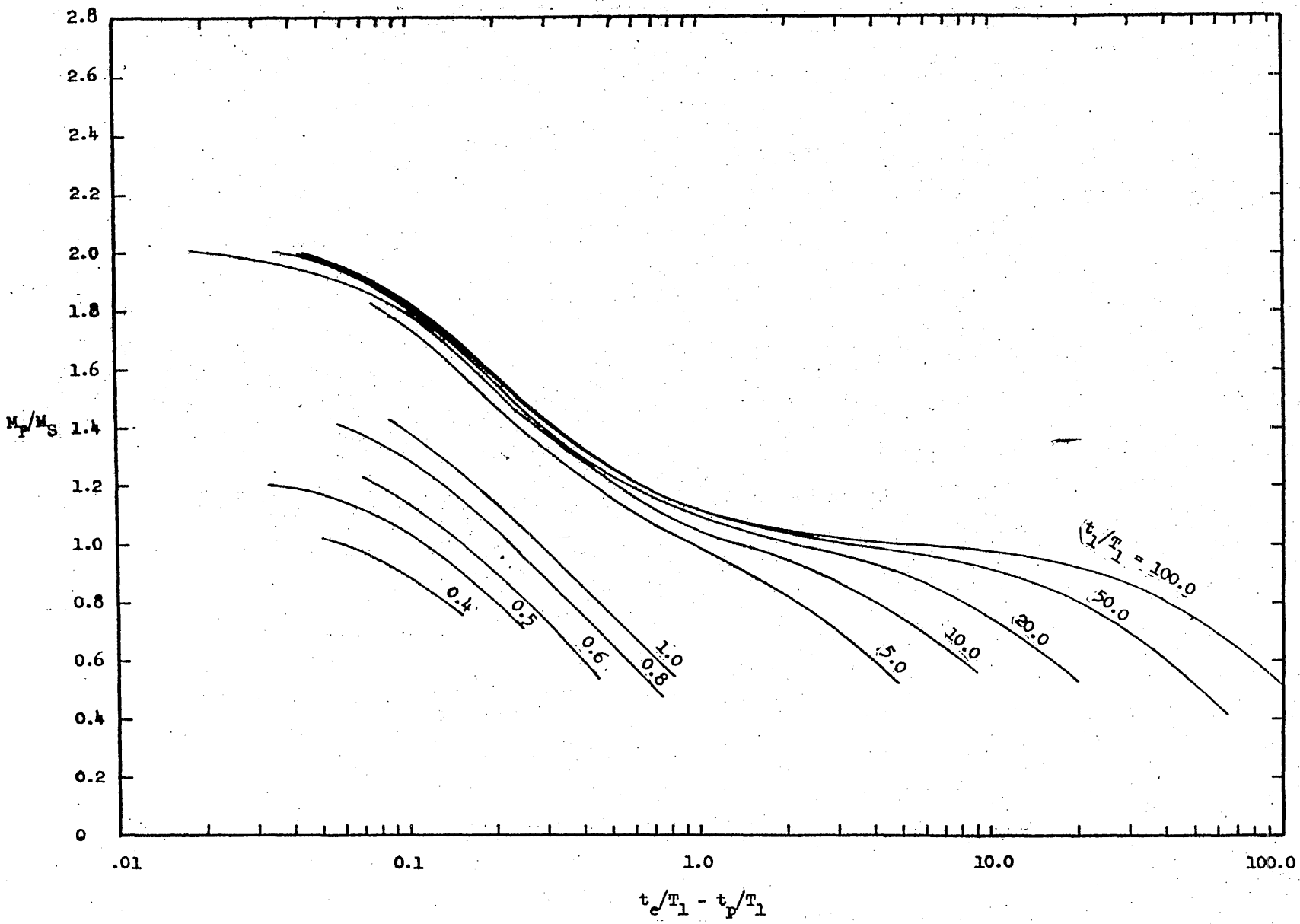

Figure 39 - Plot of Duration of Plastic Phase Versus Beam Resistance Parameter (M_P/M_S) for Fixed Values of Pulse Duration (t_1/T_1)

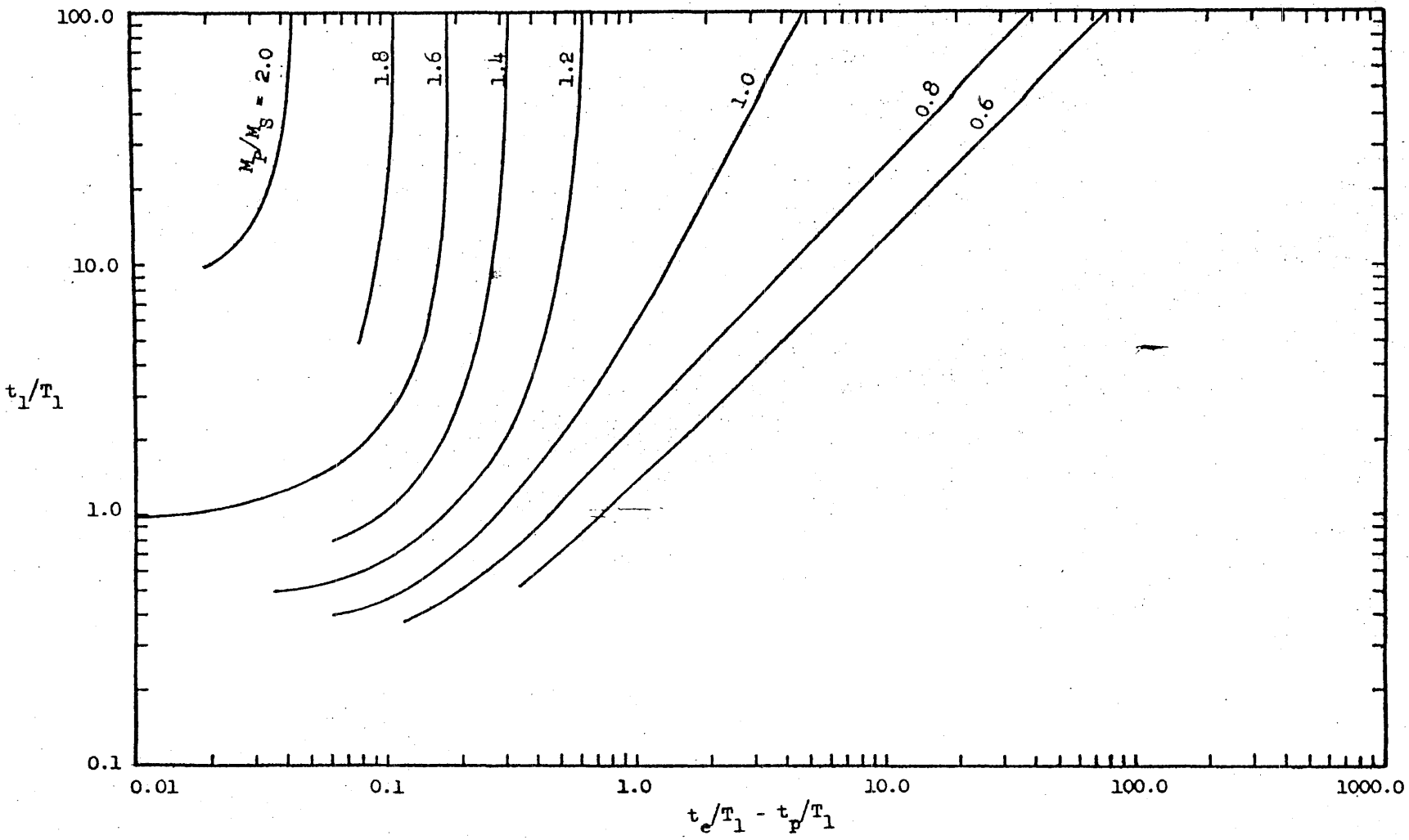

Figure 40 - Plot of Duration of Plastic Phase Versus Pulse Duration (t_1/T_1) for Fixed Values of Beam Resistance Parameter (M_P/M_S)